2023

Mechanisms of Emulsion Destabilization: An Investigation of Surfactant, Stabilizer, and Detergent Based Formulations Using Diffusing Wave Spectroscopy

JORDAN N. NOWACZYK

Mechanisms of Emulsion Destabilization: An Investigation of Surfactant, Stabilizer, and Detergent Based Formulations Using Diffusing Wave Spectroscopy

Jordan Nowaczyk

A thesis presented for the degree of
Master of Science

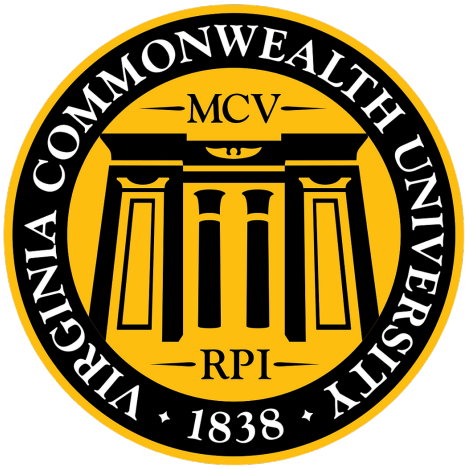

Advisor: James K. Ferri, PhD
Chemical and Life Science Engineering
Virginia Commonwealth University
Richmond VA, USA
May 2023

Contents

©

Copyright Page

Acknowledgments

The author wishes to thank several people. I would like to thank my family for love and support during my studies. I would also like to express gratitude to our research group for their assistance and direction during this project. Further, I would like to specifically thank Robert E. McMillin for expert guidance and Katie Centofante for collaboration on this work. Much appreciation to our collaborators at Afton Chemical Corporation for funding and allowing this project to be the work of my thesis. Lastly, I would like to express immense gratitude to Dr. James K. Ferri, for offering extensive knowledge, unending mentorship and direction throughout the course of my degree.

Abstract

Mechanisms of Emulsion Destabilization: An Investigation of Surfactant, Stabilizer, and Detergent Based Formulations Using Diffusing Wave Spectroscopy

A thesis submitted in partial fulfillment of the requirements for the degree of Master of Science at Virginia Commonwealth University.

By Jordan Nowaczyk

Virginia Commonwealth University, 2023

Advisor: James K. Ferri PhD, Chemical and Life Science Engineering

Conventional approaches for studying emulsions, such as microscopy and macroscopic phase tracking, present challenges when it comes to establishing detailed mechanistic descriptions of the impact of emulsifier and stabilizer additives. Additionally, while a combination of sizing methods and macroscopic phase tracking can provide insights into droplet size changes and concentration, the use of multiple measurements can be cumbersome and error-prone. It is the focus of this work, to present a new method for studying water in oil (W/O) emulsions that involves using diffusing wave spectroscopy (DWS) to examine the impact of three different surface stabilizing additives at varying concentrations. By monitoring changes in the transport mean free path length (l^*) it is demonstrated that a single DWS measurement provides similar insights to traditional methods. In addition to revealing physical dynamics inaccessible through conventional techniques. Nine specific additives were analyzed and detailed characterization and classification with relation to mechanisms of destabilization are detailed, and provide useful in improving formulations. The wealth of information provided by DWS measurements suggests that it could be useful in developing formulations tailored to specific use cases, rather than just in fundamental research.

1 Introduction

Emulsions are a specific type of mixture composed of two immiscible liquids, such as oil and water, stabilized by a third component, typically a surfactant or other emulsifying agent.[1–3] The emulsifying agent reduces interfacial tension between the two liquids allowing for the formation of a stable dispersion of droplets.[1,4,5] In emulsions, the two immiscible liquids are referred to as the disperse phase and the continuous phase. The disperse phase is the liquid, present in the form of droplets, dispersed throughout the continuous phase. Whereas, the continuous phase is the liquid that surrounds and separates the droplets of the disperse phase.[1] Use cases for emulsions are diverse and span across industry. They have proven vital in applications ranging from pharmaceuticals and personal care products, to large scale pollutant remediation processes, textile/paper processing, and in commercial products such as paints, sealants, inks, and dyes.[1,4,5] Most frequently, they are used to create desired textures, improve stability, and enhance the delivery of active ingredients.[1,4,6] The properties of the disperse and continuous phases, as well as the type and amount of emulsifying agent used, can affect the stability and properties of the emulsion. For instance, in food industry applications, the type of oil used as the disperse phase can affect the taste and texture of the final product, while the amount and type of emulsifying agent used can affect the stability and shelf life of the emulsion.[5] Further, the stability of an emulsion can be improved by controlling factors such as temperature, pH, and shear forces[1]

Emulsions are generally classified by their phase constituents, single emulsions can be either oil-in-water (O/W) or water-in-oil (W/O) depending on how the dispersion forms. For example, in a water-in-oil emulsion, water is the disperse phase and oil is the continuous phase.[4] The water droplets are dispersed throughout the continuous oil phase that surrounds and separates the water droplets, and the opposite is seen with oil-in-water emulsions. Emulsions are further classified based on thermodynamic stability. They are categorized as either macro- or micro-emulsions, where macro-emulsions are thermodynamically unstable and micro-emulsions are thermodynamically stable.[7] Typical sizes for micro-emulsions range from approximately 10-100 nm, as compared to much larger droplets exhibited with macro-emulsions, typically around 10-100 μm. Furthermore, in terms of kinetics, macroemulsions may be classified as either kinetically stable or unstable.[7]

In order to increase stability and prevent phase separation, two classes of ad-

ditives are commonly used: emulsifiers, including small molecule surfactants, and stabilizers, such as polymers.[6] Emulsion stabilization is achieved with both, but their chemical and physical mechanisms of action differ. Surfactants are typically amphiphilic molecules that reduce interfacial tension between dispersed and bulk phase via adsorption at the interface which decreases the total free energy of the system and enhances emulsification.[8] Additionally, steric and electrostatic repulsion among droplets increases, thereby inhibiting continuous phase drainage. Furthermore, at concentrations exceeding the critical micelle concentration (CMC), viscosity may increase due to micelle formation in the bulk phase.[9] Alternatively, polymers are not usually amphiphilic, so their activity is not constrained to the surface. Polymer action at the interface involves steric hindrance and modification of the momentum transfer boundary condition due to increased viscosity and friction factor, attributed to polymer adsorption.[5,10] The motion of the droplets decreases due to increased friction factor at the interface, and bulk phase creaming slows. Moreover, polymers are associated with bulk phase viscosity increases, thereby slowing diffusion of emulsion droplets.[10] Interestingly, the mechanisms of action exhibited by detergents mimic both small molecule surfactants and polymers.

In the automotive lubrication industry particular attention is paid to component manufacturing. Exploration of formulations involving additives such as advanced friction modifiers, antiwear materials, low viscosity lubricants, dispersants, antioxidants, and corrosion inhibitors is critical to satisfy stringent energy efficiency requirements and environmental legislation.[11–13] Understanding dynamics associated with these components and their role in formulations offers unique ability to tune quality, durability, and efficiency of products. Specific attention is paid to additives, such as surfactants, stabilizers, and detergents due to their role in motor oils used for maintaining engine performance and longevity. In general, these additives aid in emulsifying harmful contaminants that may form during combustion and as oil breaks down over time.[12]

During standard internal combustion engine operation, high pressure/temperature gasses exert force moving pistons up and down inside cylinder walls.[11,14] Stable, safe, and efficient automotive operation requires smooth contact between shifting equipment. Lubricating oils are the industry standard in reducing friction and wear. However, during combustion contaminants, namely water, inevitably enter the system. Due to the nature of operation, temperature fluctuates, and in low temperature conditions water condenses.[12,14] Undesirable accumulation of water occurs due to inad-

equate vapor pressure when low temperature conditions persist. Lubricating oils are also susceptible to oxidation leading to presence of small molecular weight contaminants such as aldehydes, ketones, acids and alcohols.[15] These challenges can be remedied by leveraging lubricating oil additive properties and emulsification phenomena. In the aforementioned system, the ability to suspend contaminants via water-in-oil (W/O) emulsions is imperative.

While structure and individual properties of additives are well studied, quantitative characterization of emulsion dynamics is lagging. The standard technique for evaluating lubricating oil emulsification ability is the ASTM-D7563 test, from ASTM International.[16] It is a qualitative pass/fail method in which a W/O emulsion is prepared and after 24 hours the sample is observed for the presence of aqueous layer formation. The test has several drawbacks, including large volume and lengthy time requirements.[16] Furthermore, it is inherently qualitative, making it inadequate for assessing time-resolved stability. Another method of analysis is optical microscopy. Microscopy provides a slightly elevated understanding of system behavior including droplet size and floc formation.[17] However, invasive sampling is unavoidable and limited statistics are provided. A more valuable method of characterizing emulsion behavior is Diffusing Wave Spectroscopy (DWS). DWS allows non-invasive sample interrogation in dense suspensions through quantitative time-resolved measurements and yields statistical insights about rapid phenomena.[18] It is the purpose of this work, to utilize DWS, optical microscopy, and ASTM-D7563 for examination of three common classes of additives: small molecule surfactants, stabilizers, and detergents. Three specific molecules from each of these classes is examined, revealing insights pertaining to mechanisms of destabilization, not possible with traditional methods alone. Therefore, methods presented in this work may be advantageous for application specific formulations in a broad range of industries.

1.1 Emulsion Kinetics

Emulsion droplet size aging is generally attributed to three predominant phenomena: Ostwald Ripening (OR), aggregation, and coalescence. Each of these phenomena, represented in Figure 1B, potentially increase creaming/settling. OR is a diffusionary process associated with travel of dispersed phase molecules through the bulk phase. Droplet polydispersity provides a gradient required for diffusion. Small droplets possess higher interfacial energy per volume (and Laplace pressure), so small droplet molecules will diffuse from smaller to larger droplets. OR causes large droplets to in-

crease at the expense of smaller droplets.[19] As droplet size increases, the density difference between dispersed and bulk phase increases; creaming/settling become more probable. Therefore, droplet growth from OR is often correlated with macroscopic phase separation. Alternatively, aggregation and coalescence require interaction between two or more droplets, making them dependent on diffusion/dynamics of complete droplets.[20] During aggregation, stable flocs composed of multiple droplets form and are separated by a bulk phase thin film. Effective droplet size increases and when thin films burst coalescence becomes more likely.[19] Ultimately aggregates merge to form single larger droplets. Notably, aggregation can increase the probability of coalescence, but coalescence may happen in the absence of aggregation. If droplets move with enough speed, high kinetic energy collisions cause droplets to coalesce prior to thin film formation.

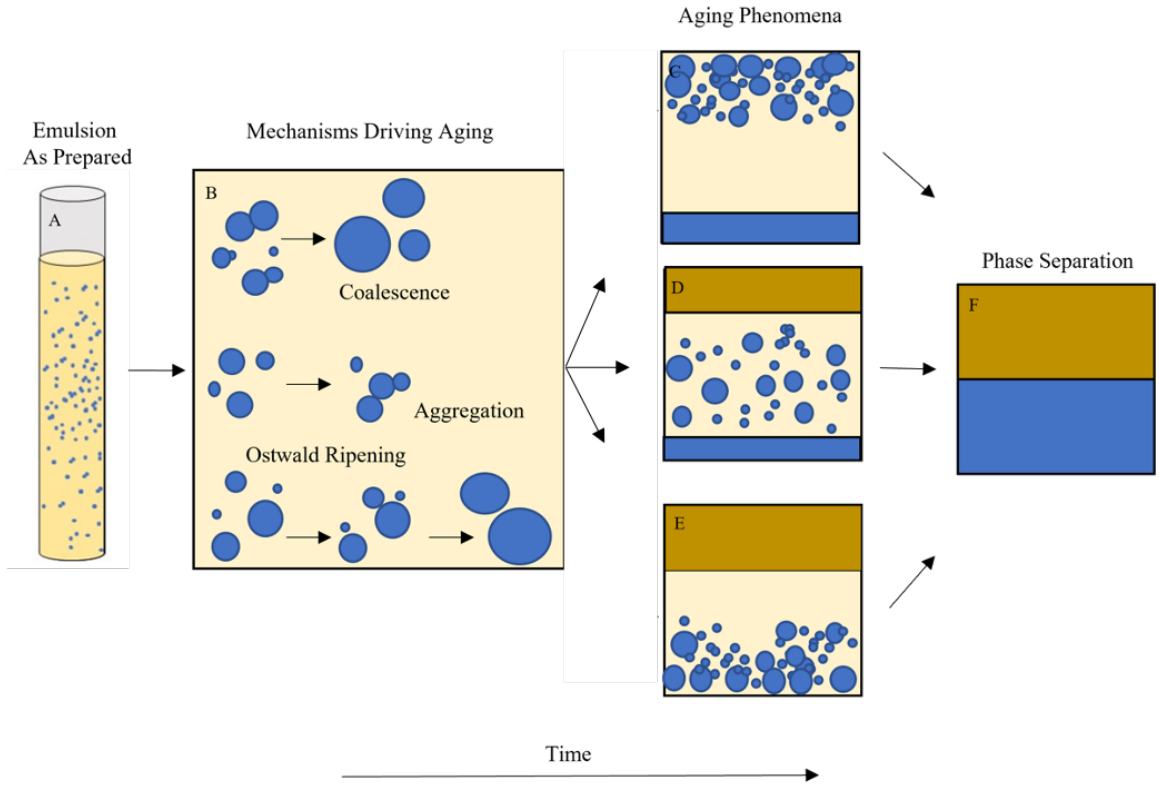

Figure 1: Ageing process of a W/O emulsion with potential mechanisms of destabilization represented A) Initial emulsion at time zero, B) Potential mechanisms (Coalescence, Aggregation, and Ostwald Ripening) contributing to destabilization depicted C) Emulsion with settled water phase D) Emulsion with a creamed oil phase and settled water phase E) Emulsion with a creamed oil phase F) Fully separated emulsion

The concentration of droplets is critical in identifying the probability of droplet interactions, a prerequisite for both aggregation and coalescence. The number density of droplets is described by $N = 3\phi/4\pi\langle a\rangle^3$, where ϕ is the volume fraction of the dispersed phase and $\langle a\rangle$ is the average effective droplet size. Therefore, change in concentration due to size is inversely proportional to $\sim \langle a\rangle^3$. A generalized rate equation, Equation 1, can be used to describe aggregation, coalescence, and OR phenomena in terms of kinetics.

$$-\frac{dN}{dt} = k_n N^n \tag{1}$$

Where N is the number density of free emulsion droplets and aggregates ($N = 3\phi/4\pi\langle a\rangle^3$) and n is the order of the process. Integration, rearrangement, and substitution for the average size of droplets/aggregates yields the following general equation describing emulsion droplet size as a function of time:

$$a(t) = \sqrt[3]{\frac{a_0^3\phi(t)}{\phi_0}}\,(1 + (n-1)k_n t)^{1/3(n-1)} \tag{2}$$

Empirical evidence suggests aggregation to be of the order $n = 3/2$ and OR to be of the order $n = 2$.[21–23] Coalescence has also been shown to be a first order process, however, Equation 2 is undefined for $n = 1$. Therefore, Eq 3, a simple exponential models coalescence behavior:[23]

$$a(t) = \sqrt[3]{\frac{a_0^3\phi(t)}{\phi_0}e^{k_c t}} \tag{3}$$

1.2 Elucidating Stabilization Mechanisms with Light Scattering

A method of emulsion stability analysis using DWS is presented in order to surmount drawbacks associated with other commonly employed techniques, as discussed in Section 1. The posited method builds upon prior work of McMillin et al..[18] The technique uses DWS to accurately size concentrated suspensions and obtain information about emulsion droplet concentration, size, and dynamics. DWS is a photon correlation spectroscopy method, similar to Diffusive Light Scattering.[18,24] Intensity fluctuations of scattered light are related to optical and dynamic properties of a sample. The general process involves coherent light penetrating a vessel containing an emulsion sample. As photons diffuse through the sample, they get scattered due to contact

with moving emulsion droplets. Finally, photons are collected by a detector in the far field. Intensity fluctuations are correlated in time yielding an intensity autocorrelation function, $g_2(\tau)$. While $g_2(\tau)$ provides some insight about the emulsion, further transformation is required to extract more detailed information. The Siegert relationship is used to transform $g_2(\tau)$ to the electric field autocorrelation function, $g_1(\tau)$. $g_1(\tau)$ is a function of experimental geometry, optical properties, such as wavelength of light, and the dynamics of the emulsion:[24]

$$g_1(\tau) = \int_0^\infty P(s) e^{-k_0^2 \langle \Delta r^2(\tau) \rangle \frac{s}{3l^*}} \, ds \tag{4}$$

The electric field autocorrelation function, $g_1(\tau)$, represented by Equation 4, is established by examining light scattering as a diffusion process. In this scenario, photons undergo a random walk of path length s, with an average step size l^*, and have a certain probability of taking that path $P(s)$. In Equation 4, k_0 is the incident wave vector, given by $k_0 = 2\pi n/\lambda$, and $\langle \Delta r^2(\tau) \rangle$ is the mean squared displacement of all scattering centers within the incident light at time τ. Both s and $P(s)$ are functions of the experimental geometry and l^*. In the simplest circumstances they have an analytical form.[25] However, numerical Monte Carlo simulations yield s and $P(s)$ distributions for situations lacking analytical forms.[18,26,27] Notably, these simulations are specific to the experimental geometry employed for a given value of l^*. Monte Carlo simulations for the experimental setup of this work were performed, as outlined by McMillin et al..[18]

The transport mean free path length, l^*, is predominantly a function of droplet size and concentration. To determine l^* independently of the mean squared displacement, a calibration process outlined by McMillin et al. is utilized. Using Mie theory, l^* is related to the average distance between scattering events, l, corrected by an anisotropy factor, $l^* = l/(1-g)$.[24,28] The mean free path, l, is a function of the distance between particles and the particles' scattering cross section and is defined as:[29]

$$l = \frac{4\langle a \rangle}{3\phi Q_s} \tag{5}$$

where $\langle a \rangle$ is the average scattering center radius, ϕ is the volume fraction of scattering centers, and Q_s is the scattering efficiency factor.[29] Q_s is a function of the average scattering center size and refractive index relative to the refractive index of the medium, and wavelength of light. By substituting Equation 5 into the l^* expression a new expression is obtained:

$$l^* = \frac{4\langle a \rangle}{3\phi Q_s(1-g)} \tag{6}$$

Contrary to the apparent linear dependence of l^* on $\langle a \rangle$, Equation 6 is much more complex; owing complexity to Q_s and g which are complicated non-linear functions of $\langle a \rangle$ that alter the scaling. Q_s and g may be determined through exhaustive calculations utilizing Mie theory for a range of droplet and continuous phase refractive indexes, sizes, and wavelengths of light.[30,31] Further, volume fractions and droplet size distributions are functions of time, therefore Equation 6 can be parameterized by substitution of $\langle a(t) \rangle, \phi(t), Q_s(a(t))$, and $g(a(t))$.[18]

The mean square displacement $\langle \Delta r^2(\tau) \rangle$ is a measure describing droplet motion in time and typically can be subdivided into three major regimes: diffusive (Brownian) motion, sub-diffusive motion, and super-diffusive motion. Droplets exhibiting diffusive motion only interact with the bulk phase and thermal fluctuation drives their motion, balanced by the friction factor at the interface. Therefore, the mean squared displacement varies directly with time and exhibits a slope inversely proportional to droplet size. In the case of a hard sphere and three dimensional diffusion, the slope is defined by the Brownian diffusion coefficient, so the mean squared displacement is $\langle \Delta r^2(\tau) \rangle = 6\frac{k_b T}{6\pi\mu\langle a \rangle}$. With super-diffusive motion, the slope scales super-linearly in time because velocity causes the average motion of droplets to be faster than with diffusion alone.[27,32] Alternatively, sub-diffusive suggests less motion than that of diffusion and is explained by droplet-droplet interactions; the mean squared displacement scales sub-linearly in time. An anomalous diffusion model is used in order to parameterize the mean squared displacements extracted from Equation 4.

$$\langle \Delta r^2(\tau) \rangle = 6K_\alpha t^\alpha \tag{7}$$

Equation 7[18,33] is fit to all extracted mean squared displacement curves by varying the parameters K_{alpha} and α. For $\alpha = 1$, K_α is the Brownian diffusion coefficient, for $\alpha < 1$ the average droplet motion is sub-diffusive, and for $\alpha > 1$ the motion is super-diffusive with a velocity variance.

2 Experimental Design

2.1 Materials

The test oils for all experiments consisted of a base oil and an additive pack provided by Afton Chemical Corporation. The additive pack contained additives such as dispersants, stabilizers, antiwears, and antioxidants in amounts mimicking that of which is found in a typical engine oil lubricant formulation. Afton Chemical Corporation also supplied E85 fuel and the nine additives analyzed, which were employed without further purification. E85 fuel consists of 85% ethanol and 15% unleaded gasoline. For all experimentation, Ultrapure (18.2 MΩ at 25 oC) water was obtained from a MilliQ dispenser.

Surfactants

A surfactant, short for surface-active agent, is a chemical substance that can reduce the surface tension between two substances, such as a liquid and a gas or two liquids. Surfactants are typically amphiphilic, meaning they have both hydrophilic (water-loving) and hydrophobic (water-repelling) properties.[8,34] The hydrophilic part of the surfactant molecule is attracted to water, while the hydrophobic part is attracted to non-polar substances, such as oils or fats. This allows surfactants to act as emulsifiers, helping to disperse or dissolve non-polar substances in water and vice versa.[34] The small molecule surfactant structures provided by Afton Chemical Corporation and are depicted in Figure 2.

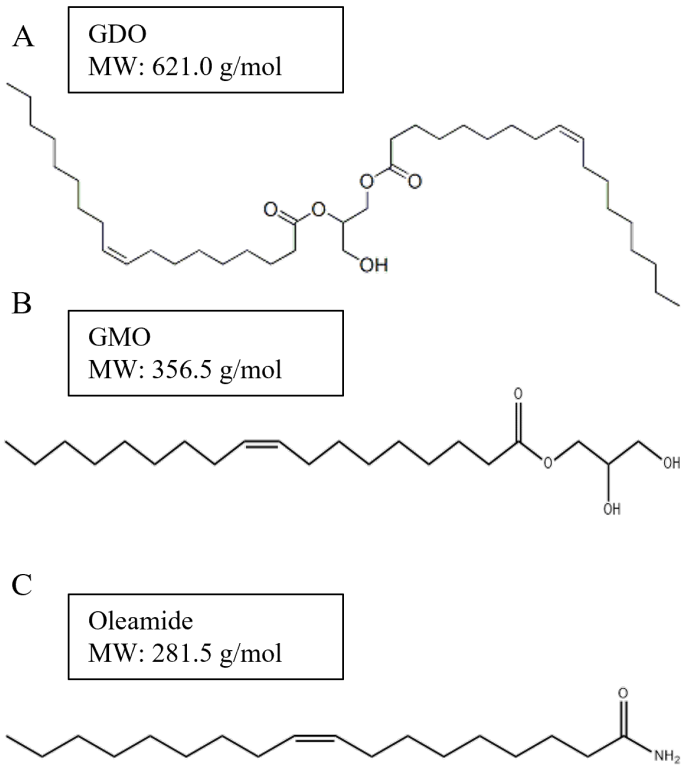

Figure 2: Generalized structure and average molecular weight of the three small molecule surfactants studied. A) glycerol dioleate (GDO) B) glycerol monooleate (GMO) C) oleamide (OA)

The three surfactants examined were glycerol dioleate (GDO), glycerol monooleate (GMO), and oleamide (OA), which were all used without further purification. The surfactants provided are mixtures and representation in Figure 2 depicts an average structure. Of note, the molecular weights of each surfactant vary and are reported in Figure 2. In observing the structures depicted in Figure 2, it is clear that there are notable differences between the small molecule surfactants. For instance, the number of oxygens differs among molecules; GDO has five oxygens, GMO has four, and OA has only one. Further, OA is the only surfactant that contains nitrogen. Each surfactant has different functional groups and properties that ultimately may dictate their performance in emulsion stability. The same concentrations based on wt% (0.1, 0.2, 0.5, 1.0 wt%) were examined in the surfactant, polymer, and detergents series. However, since we were provided structural information for the surfactants additional experiments based on molar mass were conducted. Examining the behaviors of GDO, GMO, and OA as a function of molar concentration allows one to draw conclusions on what structural properties may impact emulsion stability.

Stabilizers

There are many different kinds of stabilizers that may be used in emulsion stabilization. One class of stabilizers is polymers.[20,35] Polymers are long-chain molecules that can be used to stabilize emulsions by forming a protective layer around the dispersed droplets. This layer helps to prevent the droplets from coalescing or aggregating, which can lead to phase separation and instability of the emulsion. There are several types of polymers that may be employed.[8,20,35,36] For instance, natural polymers, such as proteins and polysaccharides, which are derived from plants or animals; examples include casein and gelatin. Synthetic polymers such as polyvinyl alcohol (PVA), polyvinylpyrrolidone (PVP), and polyethylene glycol (PEG) and polymeric surfactants.[35,37] Polymeric surfactants are typically amphiphilic molecules that contain both a hydrophobic tail and a hydrophilic head group. They are similar to small molecule surfactants, but are larger and more complex.[36,37]

For experiments analyzing stabilizer behavior in formulations, specific chemical properties and information about structure and molecular weight were not provided, due to proprietary regulations. While this type of information may enhance interpretation of results, it is certainly not required as is demonstrated by the analysis of the stabilizer series.

Detergents

detergents are another category of additives frequently applied in emulsion stabilization processes. Detergents are effective at emulsifying oily and greasy substances, by solubilizing the non-polar droplets in the aqueous phase. One of the advantages of sulfonate detergents is their excellent solubility in water, which helps to ensure uniform distribution of the detergent in the solution.[38] They are also relatively inexpensive to produce, making them a cost-effective choice for many cleaning applications.

The detergent series of this work focused on three detergents provided by Afton Chemical Corporation. The three detergents examined were Detergent 1, Detergent 2, and Detergent 3 and all were used without further purification. Table 1 reports the limited properties known about detergents supplied for investigation.

Detergent	Structure*	Appearance	Viscosity @ 100°C, cSt:	Spec Grav @ 15.6°C	Densit (lbs/gal.)	Features
Detergent 1	Highly basic calcium sulfonate Calcium, % wt.: 11.9 TBN, mg KOH/g: 307	Dark brown viscous liquid	30	1.127	9.39	High acid neutralization rate
Detergent 2	Neutral calcium sulfonate Calcium, % wt.: 2.60 Chlorine, % wt.: 0.26 TBN, mg KOH/g: 27.5 Water, % wt.: 0.3 max Sulfur, % wt.: 2.3	Dark brown viscous liquid	16	0.94	7.83	--
Detergent 3	Magnesium sulfonate Magnesium% wt. = 9.6	Brown viscous liquid	60	1.09	--	High acid neutralization rate

Table 1: detergent properties known prior to experimentation including structural information, viscosity, density, specific gravity, observed features, and general appearance

The provided information is specific to conditions as defined in Table 1 and is very limited in terms of structural detail. Exact structures and molecular weights were not provided. However, these may all be classified as a specific type of detergent, commonly known as sulfonates. Structurally, they are metal salts (either calcium or magnesium) of organic acids, containing a surface-active polar group stabilized by metallic soaps.[38,39] The polar head of the sulfonate attaches to the metal core while the hydrophobic hydrocarbon tail stabilizes the colloidal particle in the non-polar medium. The most commonly used detergents are derived from sulfonic acids. Sulfonates have the general formula $(RSO_3)_3M_y$.[39] Figure 3 depicts a general structure of a typical sulfonate detergent, not specific to any of the detergents analyzed in this work.

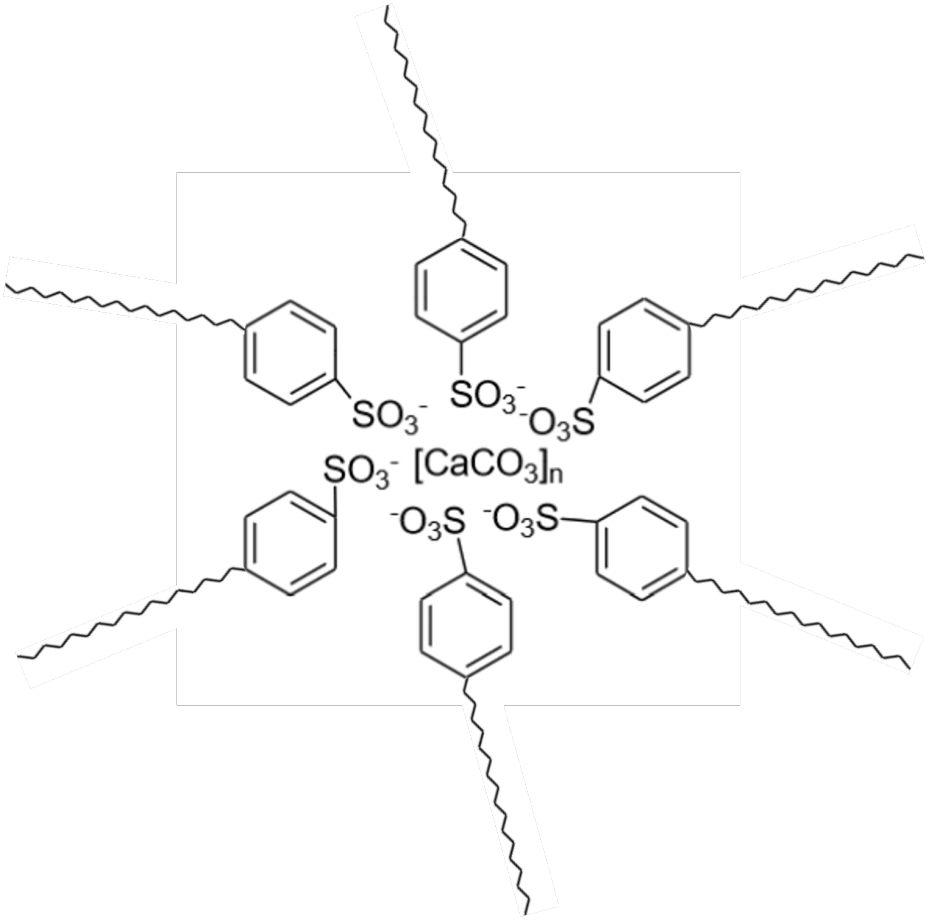

Figure 3: Generalized structure of a calcium based sulfonate detergent. The polar head from the sulfonate attaches to the calcium metal core, while the hydrocarbon tails extend toward the non-polar medium.

2.2 Emulsion Preparation

Emulsion formation was achieved by blending a 222 ml batch of oil (base oil + additive package), deionized water, and E85 fuel in an 83.3 : 8.3 : 8.3 volume ratio in a Waring blender at 10,000 RPM for 60s± 1s. Additive packages varied depending on which type of additive was being analyzed. For example, all detergent stabilized emulsions were formulated with an additive pack without detergent, all surfactant stabilized samples were formulated with an additive pack without surfactant, and all stabilizers were formulated with an additive pack without stabilizer. Each of the test oils contained one of the nine specific molecules (3 surfactants, 3 stabilizers, 3 detergents) provided by Afton Chemical Corporation. stabilizers and detergent based emulsions were formulated at four representative weight percentages: 0.1, 0.2, 0.5, and

1.0 wt%. While surfactants were analyzed at these same weight percents in addition to three molar concentrations: 3 mM, 5 mM, and 10 mM. Due to proprietary concerns detailed structural information was not provided for detergents and stabilizers, hence no formulations based on molar mass were produced. The initial volume fraction, ϕ_0 of the dispersed aqueous phase in the emulsion was calculated by summing the contribution from ethanol in the E85 fuel and water. For all formulations ϕ_0 was equal to ~ 0.154. A representative sample (3 ml) was removed from the blender via transfer pipette and deposited in two separate cylindrical sample tubes for microscopy and DWS measurements.

2.3 Microscopy

Optical analysis equipment utilized included a Nikon Eclipse E600 inverted microscope, fitted with a Nikon Plan Fluor20x/0.50 DIC M/N2 WD 2.1 objective. Images were recorded with an Imaging Source Monochrome Camera (model DMK 41AU02) connected to IC Capture 2.5 imaging software. Emulsions were stored at 25°C in 3 ml cuvettes, identical to those employed in DWS data acquisition. Aliquots were drawn from the base of the cuvettes in order to probe the layer of emulsion penetrated by the laser in DWS studies and deposited onto glass microscope slides. After deposition, the microscope slide was vertically oriented for 5 seconds to thin the sample. Droplet sizes were assessed using offline contour detection within ImageJ software. In all cases, droplets were sized until the standard deviation remained constant. Microscopy size measurements were taken every 30 minutes for the first 120 minutes post emulsification. In some cases, size determination by optical microscopy was not possible. Microscopy imaging took place over the first 120 minutes of emulsion aging for all formulations examined. Aliquots were taken and analyzed at 30 minute intervals, resulting images from t0, t30, t60, t90, and t120 are depicted in Figures 4-12 and will be referenced frequently for comparison as other methods of characterization are analyzed. These Figures 4-12 depict matrices of the micrographs obtained for each of the nine molecules investigated. Viewing micrographs in matrices, as presented, provide convenient visualization of droplet size changes as a function of laboratory time for each specific formulation (based on concentration of additive), but also allows for easier analysis of droplet size change as a function of additive concentration.

Surfactant Series Micrographs

Figure 4 shows microscopy images obtained for emulsion samples prepared with small molecule surfactant GDO as a function of laboratory time. Rows indicate concentration of formulation, from top to bottom 3 mM, 5 mM, 10 mM and columns correspond to time emulsion micrograph was obtained, from left to right: t0, t30, t60, t90, and t120. GDO formulations 3 mM, 5 mM, and 10 mM exhibit very small closely packed droplets at initial time points t0 and t30. In fact, at these early time points it is difficult to distinguish differences between the micrographs from emulsions prepared with the varying GDO concentrations (Figure 4,rows 1-3 columns 1-2). However, as time progresses emulsion behavior in the three formulations appears to diverge. GDO 3 mM shows the least change in droplet size, as evidenced by the similarity between the t120 micrograph and the t0 image.

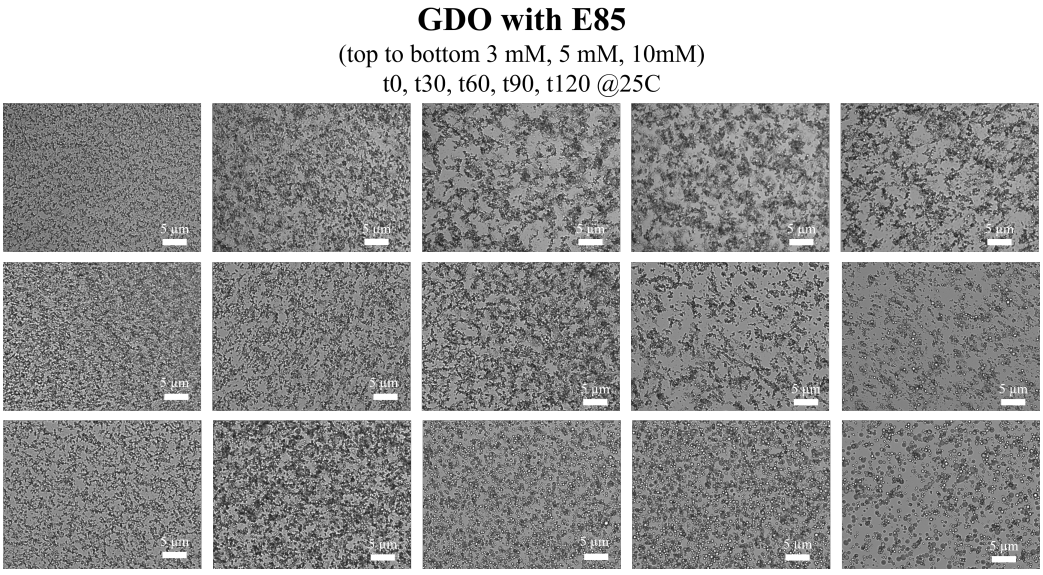

Figure 4: Microscopy images obtained for emulsion samples prepared with small molecule surfactant GDO as a function of time. Rows indicate concentration of formulation, from top to bottom 3 mM, 5 mM, 10 mM. Columns indicate time, left to right: t0, t30, t60, t90, and t120

The 5 mM GDO formulation showed similar results as the 3 mM, but at 120 minutes more distinct larger droplets appeared. Even more evident and at earlier time, is the appearance of larger distinct droplets for the 10 mM GDO formulation (Figure 4, row 3). At this concentration droplets appear clearly at 60 minutes and grow in time until the last measurement at 120 minutes. Through observing all these micrographs in concert, it can be inferred that increasing concentration of GDO leads

to faster destabilization.

Figure 5 shows microscopy images obtained for emulsion samples prepared with small molecule surfactant GMO as a function of laboratory time. Rows indicate concentration of formulation, from top to bottom 3 mM, 5 mM, 10 mM and columns correspond to time emulsion micrograph was obtained, from left to right: t0, t30, t60, t90, and t120. Micrographs obtained for GMO samples show a greater variation between the different concentrations studied than observed with GDO formulations. At 3 mM (Figure 5, row 1) droplets are very small and seem stable, a minimal amount of droplet size change is seen over the 120 minutes. Whereas, 5 mM GDO (Figure 5, row 3) shows more growth when compared to 3 mM, and much less than the droplet size evolution/growth exhibited by 10 mM GMO formulation (Figure 5, row 3). Evidenced by the size of droplets at 30 minutes, the 10 mM GMO formulation seems to destabilize quicker than lower GMO concentration samples, and even faster than the 10 mM GDO formulation discussed previously.

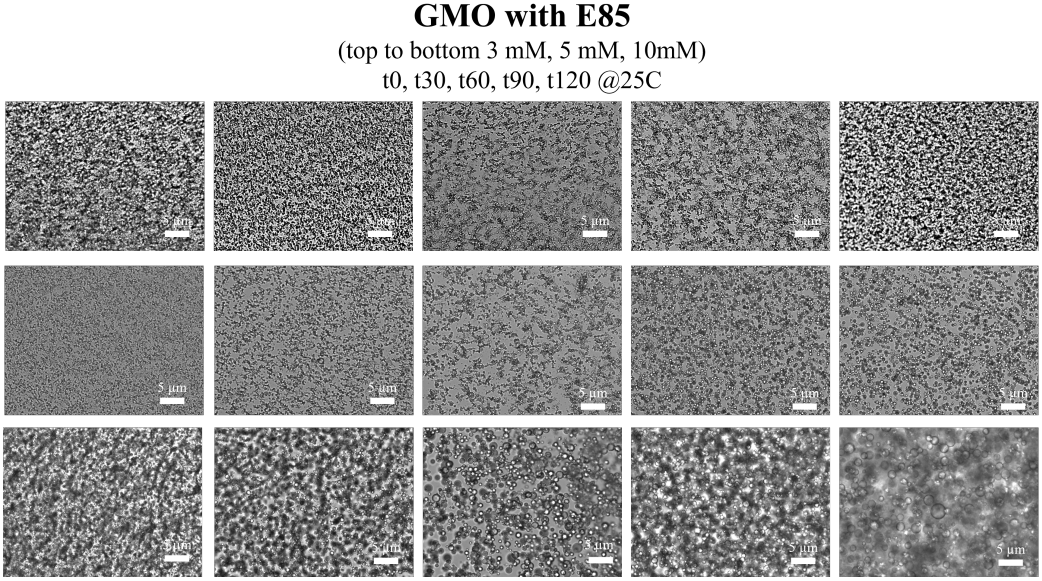

Figure 5: Microscopy images obtained for emulsion samples prepared with small molecule surfactant GMO as a function of time. Rows indicate concentration of formulation, from top to bottom 3 mM, 5 mM, and 10 mM. Columns indicate time, left to right: t0, t30, t60, t90, and t120

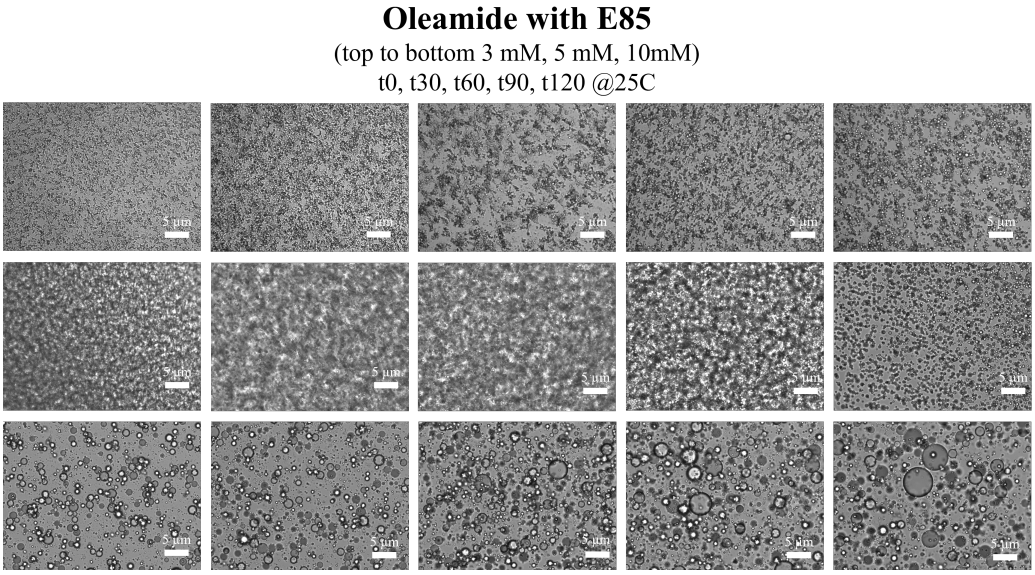

Figure 6: Microscopy images obtained for emulsion samples prepared with small molecule surfactant Oleamide as a function of time. Rows indicate concentration of formulation, from top to bottom 3 mM, 5 mM, and 10 mM. Columns indicate time, left to right: t0, t30, t60, t90, and t120

Figure 6 presents microscopy images obtained for samples containing small molecule surfactant OA as a function of laboratory time post emulsification. Rows indicate concentration of formulation, from top to bottom 3 mM, 5 mM, 10 mM and columns correspond to time emulsion micrograph was obtained, from left to right: t0, t30, t60, t90, and t120. OA micrographs reveal that, of the three small molecule surfactants investigated, OA may have the least ability to stabilize, and similar to GMO and GDO stabilizing effects are concentration dependent. Figure 6, row 1 shows that at initial times t0 and t30 droplets are small and stable, but by 60 minutes droplets are much more notable. Further, at 5 mM Figure 6, row 2 droplets are perceptible after just 30 minutes of aging and continue to grow as time progresses. Lastly and most drastically, 10 mM OA formulation micrographs reveal resolved large drops at initial time t0; by 120 minutes droplet sizes are double the size of droplets exhibited at the same time point for lower concentration OA samples.

Stabilizer Series Micrographs

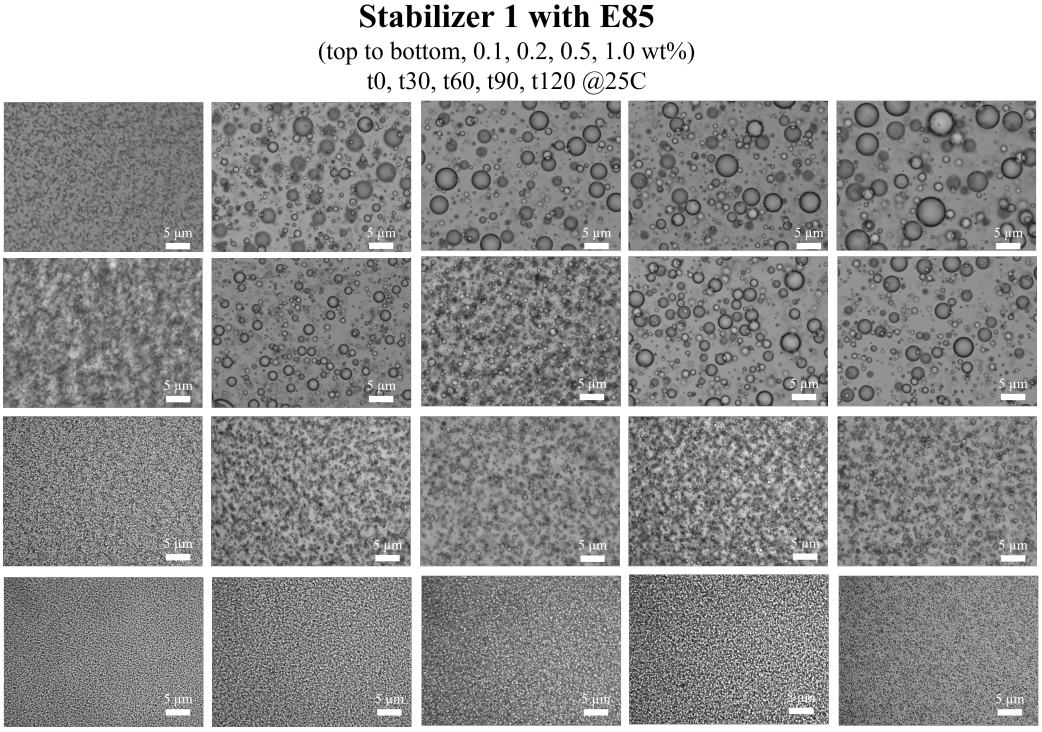

Figure 7: Microscopy images obtained for emulsion samples prepared with Stabilizer 1 as a function of time. Rows indicate concentration of formulation, from top to bottom: 0.1 wt%, 0.2 wt%, 0.5 wt%, and 1.0 wt%. Columns indicate time, left to right: t0, t30, t60, t90, and t120

Figure 7 depicts matrix of microscopy images obtained for samples containing Stabilizer 1 as a function of laboratory time post emulsification. Rows indicate concentration of formulation, from top to bottom 0.1, 0.2, 0.5, 1.0 wt% and columns correspond to time emulsion micrograph was obtained, from left to right: t0, t30, t60, t90, and t120. All prepared samples with the various concentrations of Stabilizer 1 appeared to initially exhibit sufficient drop size suppression, supported by the very small droplets visible in Figure 7, column 1. However, at the lowest concentration, 0.1 wt% (Figure 7, row 1) this quickly changes, and at 30 minutes droplet size significantly increases, with some droplets measuring approximately 3 μm. Observing this formulation age in time shows droplet size growth and at 120 minutes very resolved large droplets are imaged. Concentration 0.2 wt% follows a similar pattern albeit less dramatic. At 0.5 wt% better droplet size growth restriction is observed and at 120 minutes drop sizes are significantly smaller than those observed with 0.1 wt% and 0.2 wt%. However, as expected, droplet size still appears to slowly increase over the two hours. Most inter-

estingly, Figure 7, row 4 demonstrates that at 1.0 wt% drop sizes remain very small and are controlled over the course of aging. This likely indicates sufficient Stabilizer 1 concentration was reached.

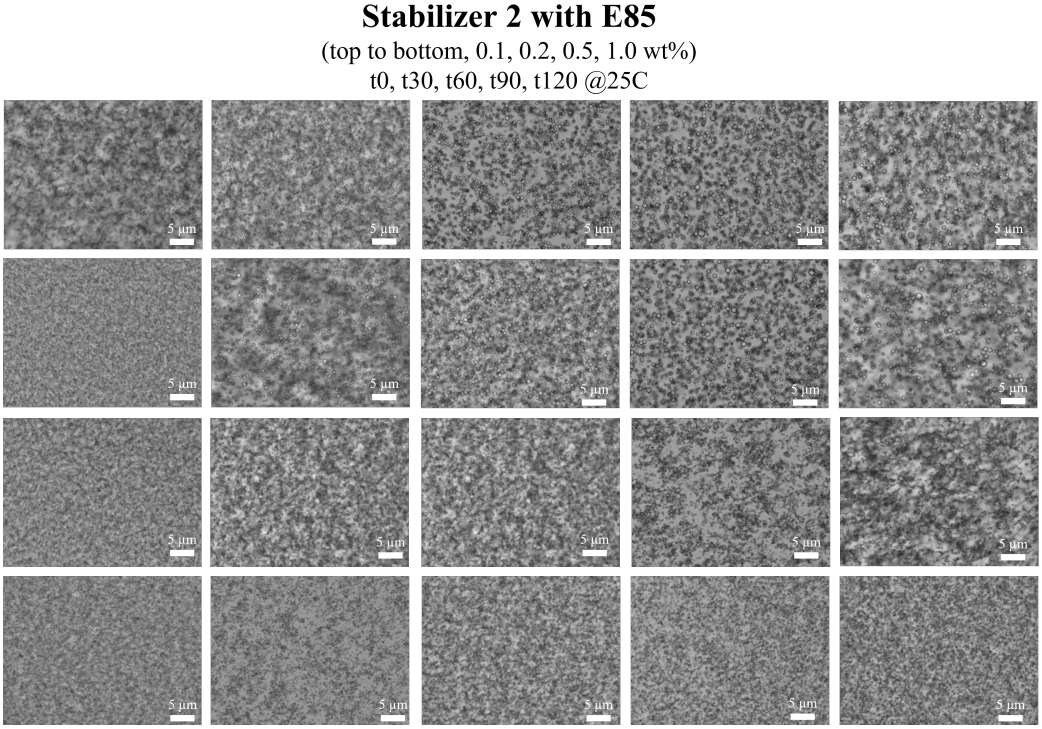

Figure 8: Microscopy images obtained for emulsion samples prepared with Stabilizer 2 as a function of time. Rows indicate concentration of formulation, from top to bottom: 0.1 wt%, 0.2 wt%, 0.5 wt%, and 1.0 wt%. Columns indicate time, left to right: t0, t30, t60, t90, and t120

Figure 8 presents microscopy images obtained for emulsion samples prepared with Stabilizer 2 as a function of laboratory time. Rows correlate to concentration of formulation, from top to bottom 0.1, 0.2, 0.5, 1.0 wt% and columns correspond to the time emulsion micrograph was obtained, from left to right: t0, t30, t60, t90, and t120. Similar to Stabilizer 1, all Stabilizer 2 formulations appeared to initially exhibit sufficient drop size suppression, supported by the very small droplets visible in Figure 8, column 1. After the initial micrographs at t0, overall contrast in trends is observed between the lower two concentrations and the higher concentrations. Dynamics in 0.1 wt% and 0.2 wt% formulations forced the formation of larger droplets during the first 30 minutes post emulsification. However, these droplets are still smaller than those of Stabilizer 1 at comparable concentrations. While, at 0.5 wt% and 1.0 wt% droplet size and patterns are comparable and no significant growth is observed. This

may indicate that increasing Stabilizer 2 above 0.5 wt% provides diminishing return.

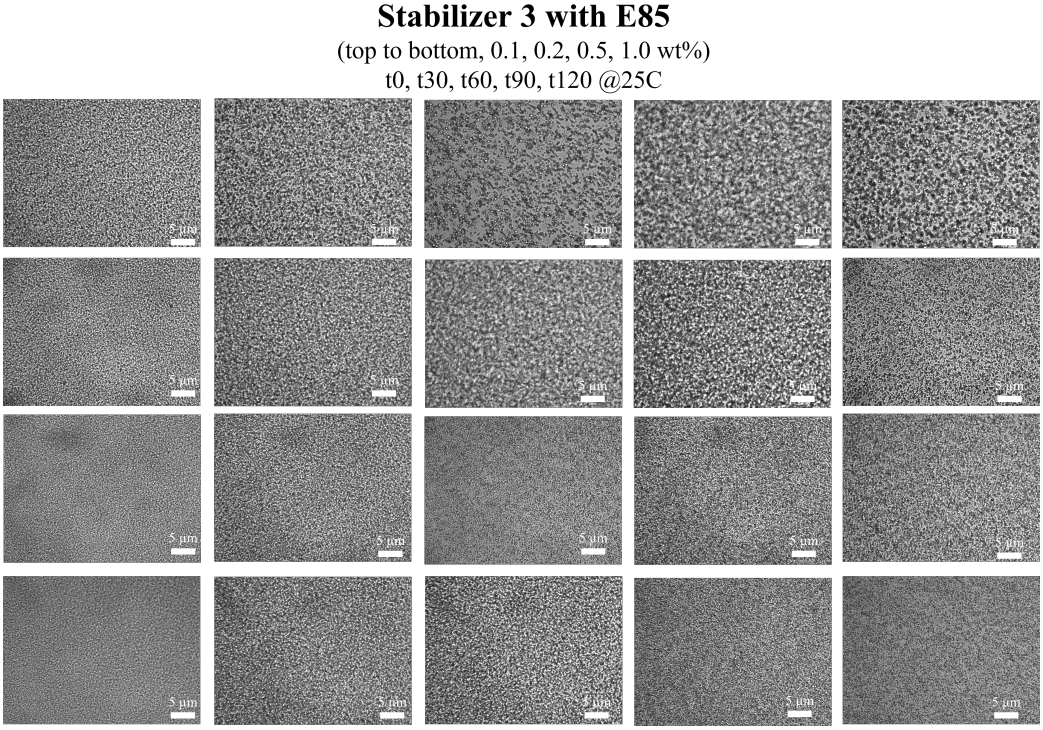

Figure 9: Microscopy images obtained for emulsion samples prepared with Stabilizer 3 as a function of time. Rows indicate concentration of formulation, from top to bottom: 0.1 wt%, 0.2 wt%, 0.5 wt%, and 1.0 wt%. Columns indicate time, left to right: t0, t30, t60, t90, and t120

Figure 9 represents emulsion aging for Stabilizer 3 formulations via microscopy images obtained as a function of laboratory time. Rows indicate concentration of formulation, from top to bottom 0.1, 0.2, 0.5, 1.0 wt% and columns correspond to time emulsion micrograph was obtained, from left to right: t0, t30, t60, t90, and t120Stabilizer 3 behavior was similar to stabilizers 1 and 2 in that droplet stabilization increased with concentration. As evident in Figure 9, column 1 droplets at all concentrations are initially very small and uniformly spread in very dense suspensions. However, at 30 minutes 0.1 wt% Stabilizer 3 formulation begins to exhibit distinguishable drops that slowly and mildly grow in time. The same trend is seen with the 0.2 wt% Stabilizer 3 sample, but the droplet growth is slightlty delayed, seeming to begin around 60 minutes. As observed with Stabilizer 2, 0.5 and 1.0 wt% formulations provided analogous micrographs during the 120 minute time course examined.

Detergent Series Micrographs

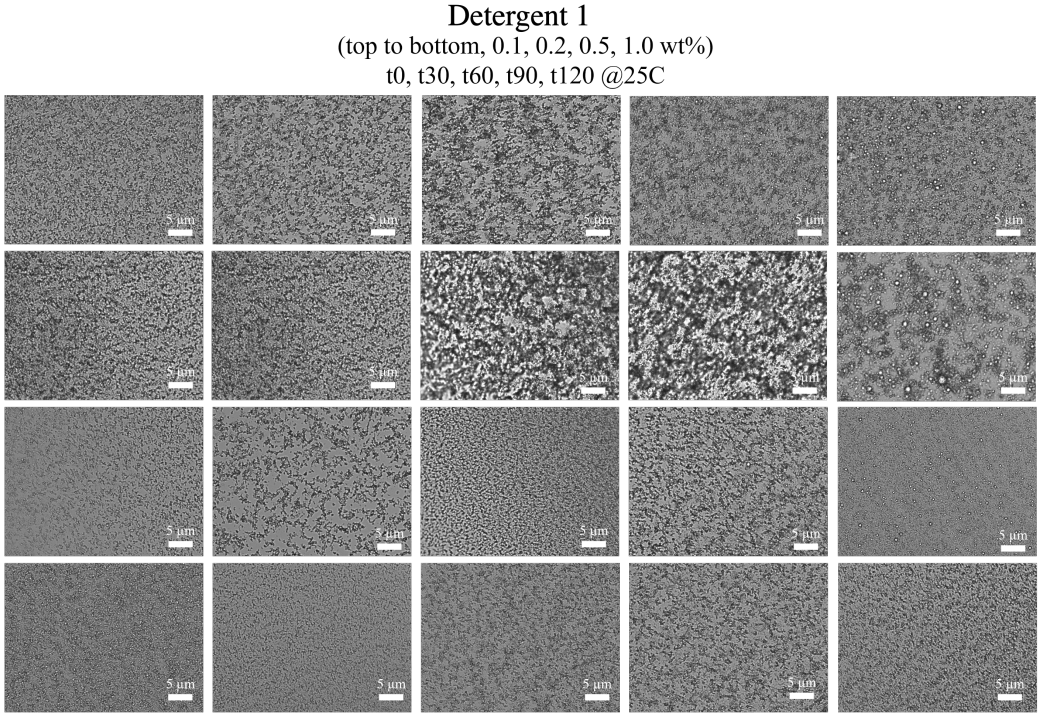

Figure 10: Microscopy images obtained for emulsion samples prepared with detergent Detergent 1 as a function of time. Rows indicate concentration of formulation, from top to bottom: 0.1 wt%, 0.2 wt%, 0.5 wt%, and 1.0 wt%. Columns indicate time, left to right: t0, t30, t60, t90, and t120

Figure 10 depicts a matrix of microscopy images obtained for samples containing detergent Detergent 1 as a function of laboratory time post emulsification. Rows indicate concentration of formulation, from top to bottom 0.1, 0.2, 0.5, 1.0 wt% and columns correspond to time emulsion micrograph was obtained, from left to right: t0, t30, t60, t90, and t120. Overall, Detergent 1 exhibited gradually increasing stabilization abilities with increasing concentration, this is evidenced best by observing Figure 10, column 5. Here it shown that presence of Detergent 1 provided some sort of stabilizing support, as droplet size decreases notably with increasing concentration. Detergent 1 0.5 wt% formulation behavior is very similar to Detergent 1 1.0 wt% at early times, showing small comparable droplets. However, after about 90 minutes 0.5 wt% begins to exhibit more defined droplet formation than 1.0 wt%. Albeit these droplets are still smaller than those observed with lower Detergent 1 concentration formulations.

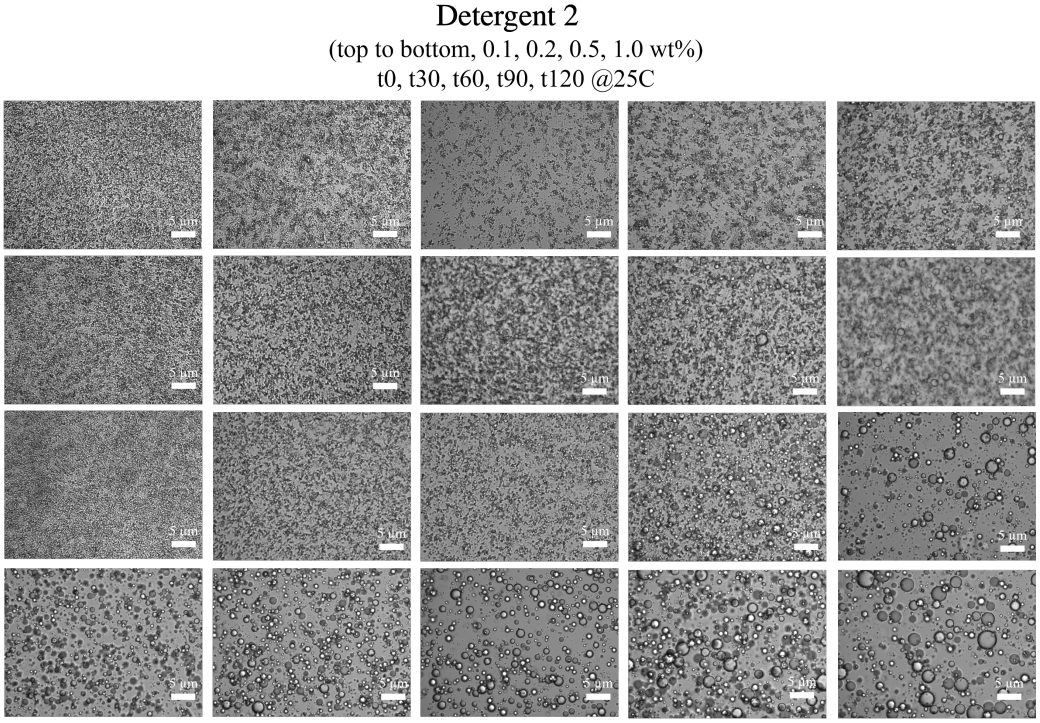

Figure 11: Microscopy images obtained for emulsion samples prepared with detergent Detergent 2 as a function of time. Rows indicate concentration of formulation, from top to bottom: 0.1 wt%, 0.2 wt%, 0.5 wt%, and 1.0 wt%. Columns indicate time, left to right: t0, t30, t60, t90, and t120

Figure 11 presents microscopy images obtained for samples containing detergent Detergent 2 as a function of laboratory time post emulsification. Rows indicate concentration of formulation, from top to bottom 0.1, 0.2, 0.5, 1.0 wt% and columns correspond to time emulsion micrograph was obtained, from left to right: t0, t30, t60, t90, and t120. Interestingly, Detergent 2 at the highest concentration 1.0 wt% showed relatively large droplets immediately after emulsification. This same behavior was observed with the surfactant OA (Figure 6, row 3). In general, the four concentrations (Figure 11, rows 1-4) exhibited progressive droplet size growth over the course of 120 minutes laboratory aging. Additionally, when comparing droplet size as a function of concentration (i.e. at specific time points, looking down a column) drop sizes gradually increase with concentration. This graduated incremental growth was more notable in the Detergent 2 formulations than with all other molecules investigated.

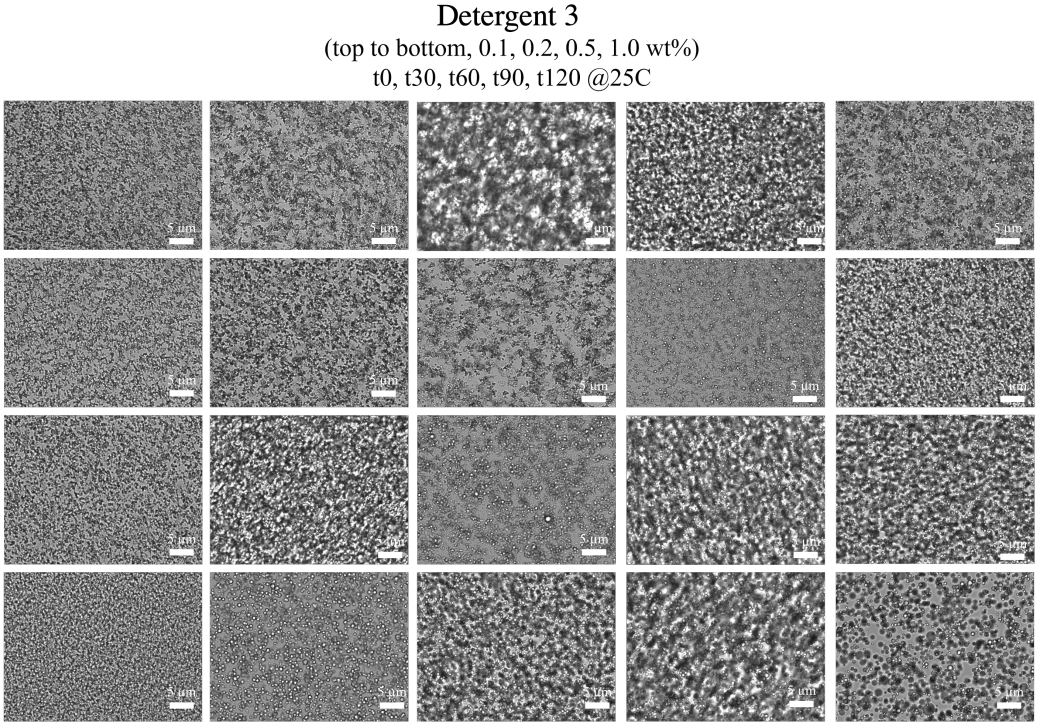

Figure 12: Microscopy images obtained for emulsion samples prepared with detergent Detergent 3 as a function of time. Rows indicate concentration of formulation, from top to bottom: 0.1 wt%, 0.2 wt%, 0.5 wt%, and 1.0 wt%. Columns indicate time, left to right: t0, t30, t60, t90, and t120

Figure 12 shows microscopy imaging captured for samples containing detergent Detergent 3 as a function of time, over the 120 minutes post emulsification. Each row indicates the concentration of formulation, from top to bottom 0.1, 0.2, 0.5, 1.0 wt% and the columns correlate with the time emulsion was sampled and micrograph was obtained, from left to right: t0, t30, t60, t90, and t120. Overall, Detergent 3 micrographs mimicked behavior observed with Detergent 2. For instance, decreasing stabilization with increasing detergent concentration is noted. However, when compared to Detergent 2, Detergent 3 showed smaller drops across the board, but especially at initial time points. This is most obvious at 1.0 wt% t0 (Figure 12, row 4-column 1). This suggests Detergent 3 provides slightly greater stabilization than Detergent 2.

Generally speaking, the stabilizers showed an inverse stabilization trend compared to the surfactants. As stabilizer concentration increases, droplet growth suppression is observed. Alternatively, droplet sizes and destabilization increases with surfactant concentration. When analyzing the detergent series microscopy, it is noteworthy that Detergent 1 follows stabilization trends similar to the stabilizers. Whereas, Detergent

2 and Detergent 3 behavior and series of micrographs are more comparable to those of the surfactant series. It should be mentioned, microscopy is undoubtedly a limited method of characterization and is inherently invasive. It is difficult to establish size and draw meaningful conclusions about small droplets in such dense suspensions, as shown in many of the micrographs presented in this work. However, by comparing micrographs in series such as those presented in Figures 4 - 12 formulators may obtain valuable qualitative insights about emulsion aging trends.

2.4 DWS

An ALV/CGS-3 Compact Goniometer from ALV-GmbH, equipped with a vertically polarized 633 nm 22 mW laser, two APD single-photon counters, an optical attenuator, and an ALV/LSE-5004 multiple τ correlator was used for all diffusing wave spectroscopy experiments. Cylindrical sample cuvettes for the instrument had an outer diameter of $\sim$ 10 mm and an inner diameter of $\sim$ 8.66 mm. The DWS workflow was developed and an in depth description was reported in prior work.[18] For the purpose of understanding this study, it is briefly described. For a single DWS experiment, a sample cuvette with the dimensions outlined above is fully filled ($\sim$3.5 ml). The intensity autocorrelation function, g_2, and the average intensity are determined over a 30 second period at detector angles of 30, 60, and 90 degrees. DWS measurements were performed every 15 minutes over the first 120 minutes post emulsification. Through utilizing a calibration process outlined by McMillin et al.[18] and the obtained average intensity, l^* at the time of sample measurement is determined. Furthermore, average intensity and a method developed by Schätzel,[40] are used to determine the theoretical variance on the intensity autocorrelation function. The Siegert relationship is used for error propagation and g_2 is converted to g_1. Mean square displacement with propagated error is extracted by using the l^* determined via intensity, and a numerical inversion of Equation 4. The mean squared displacement is further analyzed by the anomalous diffusion equation, as outlined in Section 1.2. Evidenced by Equation 4, an accurate size determination requires accurate value of l^*.

2.5 ASTM Test

The industry standard ASTM D7563 test was performed for all sample formulations examined. The process involved storing 100 mls of the prepared emulsion sample in

a 100 ml graduated cylinder undisturbed in an incubator at room temperature (20 C - 25 C) for 24 hours. The volume of each phase; oil, emulsion, and water were reported and the remaining volume fraction of the dispersed aqueous phase in the emulsion was determined. If at 24 hours, an aqueous layer formed the formulation fails the ASTM D7563 test. Figure 13A provides a schematic representation of the ASTM D7563 test, and Figure 13B reports the ASTM test results for all surfactant formulations examined.[16] Volume of emulsion remaining at 24 hours is expressed as a percent of initial volume.

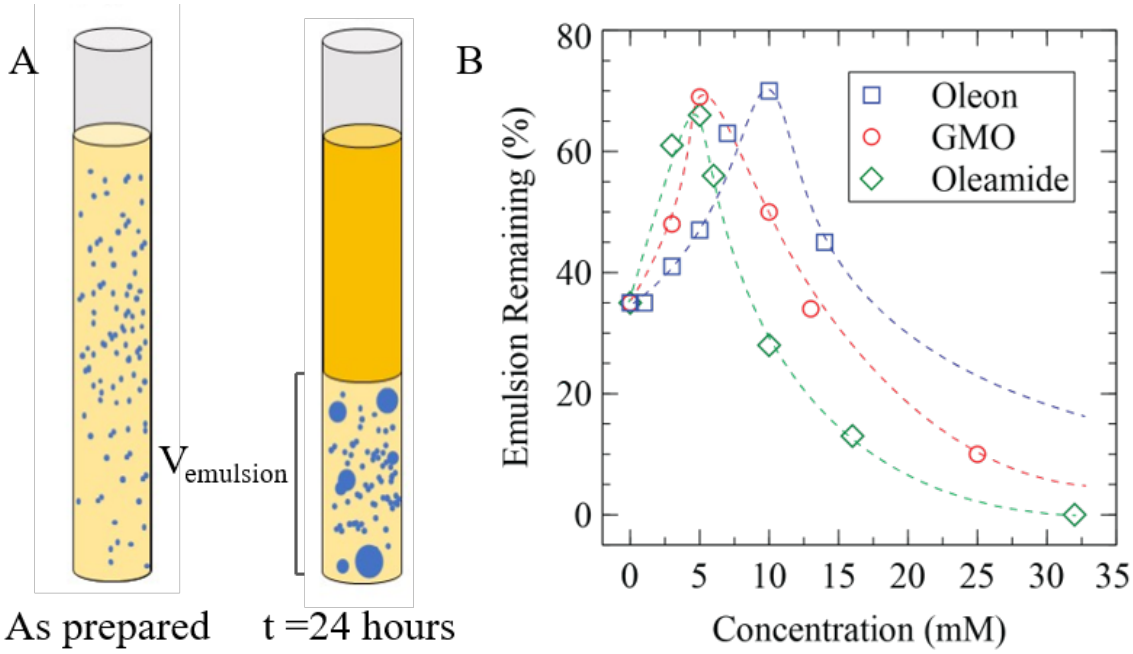

Figure 13: ASTM D7563 results for emulsions treated with small molecule surfactant. A) Schematic overview of the ASTM D7563 test. B) Emulsion remaining expressed as a percent of initial volume. Dashed lines are provided to guide the eye

For all small molecule surfactants examined, a maximum occurred around 70% of emulsion remaining after 24 hours. In emulsions prepared with GMO and OA, which have similar tail groups (shown in Figure 2), the maximum occurred when the concentration was around 5 mM. In contrast, emulsions formulated with GDO displayed a maximum stability at a concentration of 10 mM. Therefore, the delayed stabilization as a function of concentration exhibited by GDO is likely due to the increased size of the tail group.

The same ASTM D7563 test was conducted for stabilizers and detergent experi-

ments but concentration is reported by wt%. Figures 14A and 15A show the volume of emulsion after 24 hours for stabilizers and detergents at 0.1, 0.2, 0.5 and 1.0 wt% concentrations. The emulsion volume can range between 0 ml, denoting full emulsion separation over 24 hours, and 100 ml, denoting no separation over 24 hours. If a drained water layer does not appear, a lower volume of emulsion will generally indicate a higher concentration of droplets, provided the droplet sizes have not drastically increased, since the volume of water is conserved. In Figures 14B and 15B, the volume fraction of water (dispersed phase) remaining in the emulsion layer, $\phi(t)$, is shown for the corresponding experiments in Figures 14A and 15A.

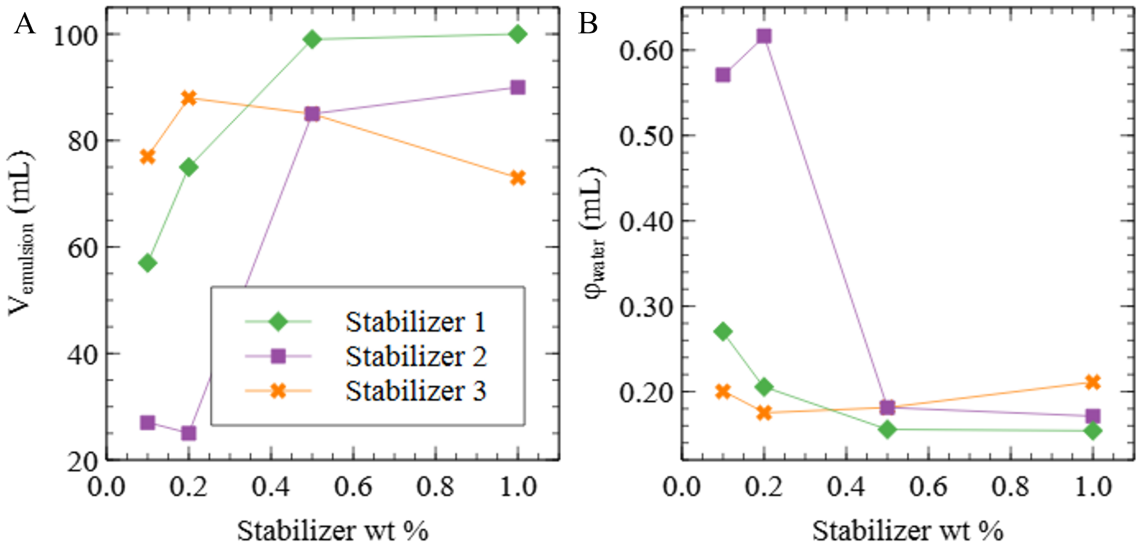

Figure 14: ASTM D7563 test results for standard formulation containing one of the three stabilizers of interest at 0.1, 0.2, 0.5 and 1.0 wt%. A) Volume of emulsion after 24 hours as a function of stabilizer concentration. B) Volume fraction of water within the emulsion phase after 24 hours as a function of stabilizer concentration.

From Figure 14A, it is implied that Stabilizer 1 has a monotonically increasing macroscopic phase-stability profile from 0.1 to 1.0 wt%. However, from 0.5 wt% to 1.0 wt% there is minimal phase-stability increase, as the emulsion volume is largely unchanged after 24 hours at both concentrations. Stabilizers 2 and 3, however, show a non-monotonically increasing phase-stability profile over 0.1 to 1.0 wt%. Stabilizer 2 had a small phase-destabilizing effect from 0.1 to 0.2 wt%, before greatly increasing phase-stability from 0.2 to 0.5 wt%. The large jump in phase-stability implies a critical concentration was met. Lastly, Stabilizer 3 displayed an increase in phase-

stability from 0.1 to 0.2 wt%; however, at concentrations greater than 0.2 wt%, phase-destabilization occurred. The phase destabilization exhibited with ASTM results in the stabilizer experiments was not observed with detergent formulations. In Figure 15, it is evident that all formulations, irrespective of which sulfonate detergent was tested, exhibit monotonically increasing macroscopic phase-stability profiles at the concentrations studied: 0.1, 0.2, 0.5, and 1.0 wt%.

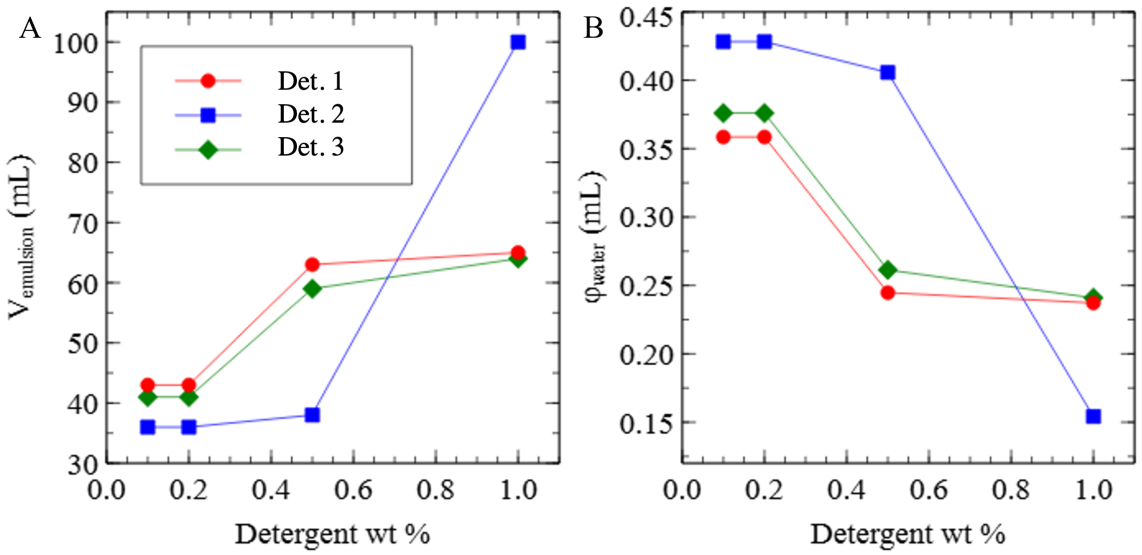

Figure 15: ASTM D7563 test results for standard formulation containing one of the three detergents of interest at 0.1, 0.2, 0.5 and 1.0 wt%. A) Volume of emulsion after 24 hours as a function of detergent concentration. B) Volume fraction of water within the emulsion phase after 24 hours as a function of detergent concentration.

For each of the detergents, as concentration increased from 0.1 to 0.2 wt%, phase stability was effectively unchanged, as the emulsion volume is largely the same at 24 hours. Furthermore, at these concentrations the phase stability effects of each detergent are comparable, with approximately 40 ml emulsion present at 24 hours. However, at 0.5 wt% Detergent 2 and Detergent 3 show marked increase before plateauing. The large jump in phase-stability implies a critical concentration was met, but above 0.5 wt% little increased stability is observed with increasing concentration. Interestingly, formulations with these two detergents Detergent 2 and Detergent 3, at all four concentrations are almost indistinguishable. Alternatively, Detergent 1 shows modest incremental increase in stabilization from 0.1 to 0.5 wt%, and then a dramatic rise in stability at 1.0 wt%. In fact, formulations containing 1.0 wt% Detergent 1 exhibited

maximum phase stabilization, indicated by 100 ml emulsion present at 24 hours.

As previously discussed, tracking the macroscopic phases of an emulsion over time provides minimal insight into the dominating mechanisms of destabilization. As a case in point, W/O emulsion phase separation of the dispersed phase typically occurs due to effective droplet size increases, but size increases can be credited to coalescence, aggregation, or OR, and differentiation between these mechanism is not possible with ASTM D7563.

3 Results

3.1 Surfactant Results

The size, optical properties such as refractive index, and concentration of emulsion droplets are all factors that contribute to the determination of the transport mean free path length, denoted as l^*, as discussed in Section 1.2. Consequently, this parameter provides crucial insights into the dynamics during the aging of emulsion samples. For the surfactants, there appeared to be an inverse relationship between molar concentration and stability. Therefore the three surfactants were assessed at comparable molarities of 3 mM, 5 mM, and 10 mM. For each emulsion formulation, DWS measurements were taken every 15 minutes for the initial 2 hours post emulsification. The transport mean free path length for the initial 2 hours with theoretical droplet growth models for each formulation are shown in Figures 16-18.

GDO Formulations

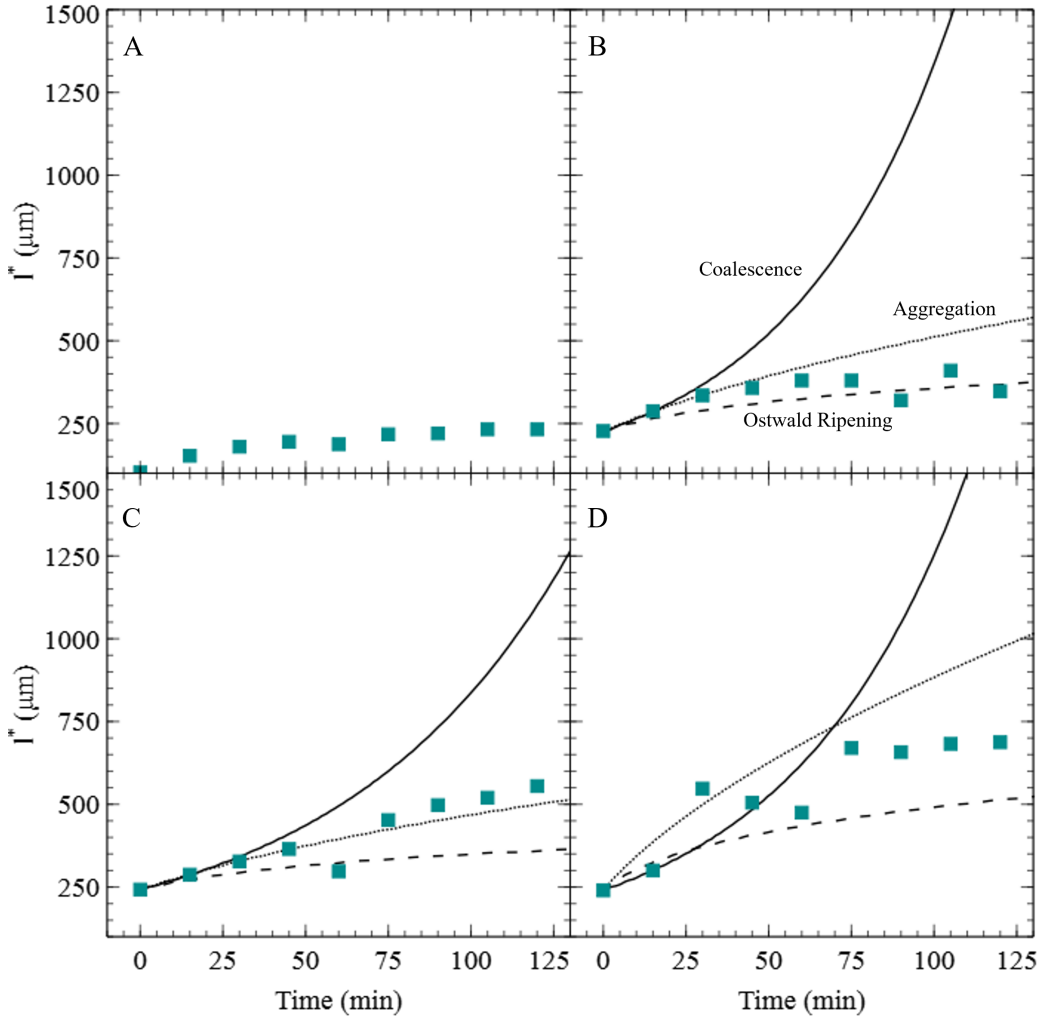

Figure 16: Transport mean free path, l^*, as a function of lab time over 120 minutes, theoretical coalescence (solid lines), aggregation (dotted lines), and Ostwald ripening (dashed lines) kinetics, for control and emulsions prepared with GDO at 3 mM, 5 mM and 10 mM. A) l^* over lab time for a control emulsion formulation, concentration of GDO is 0 mM B) l^* over lab time for an emulsion with 3 mM GDO C) l^* over lab time for an emulsion with 5 mM GDO D) l^* over lab time for an emulsion with 10 mM GDO

GMO Formulations

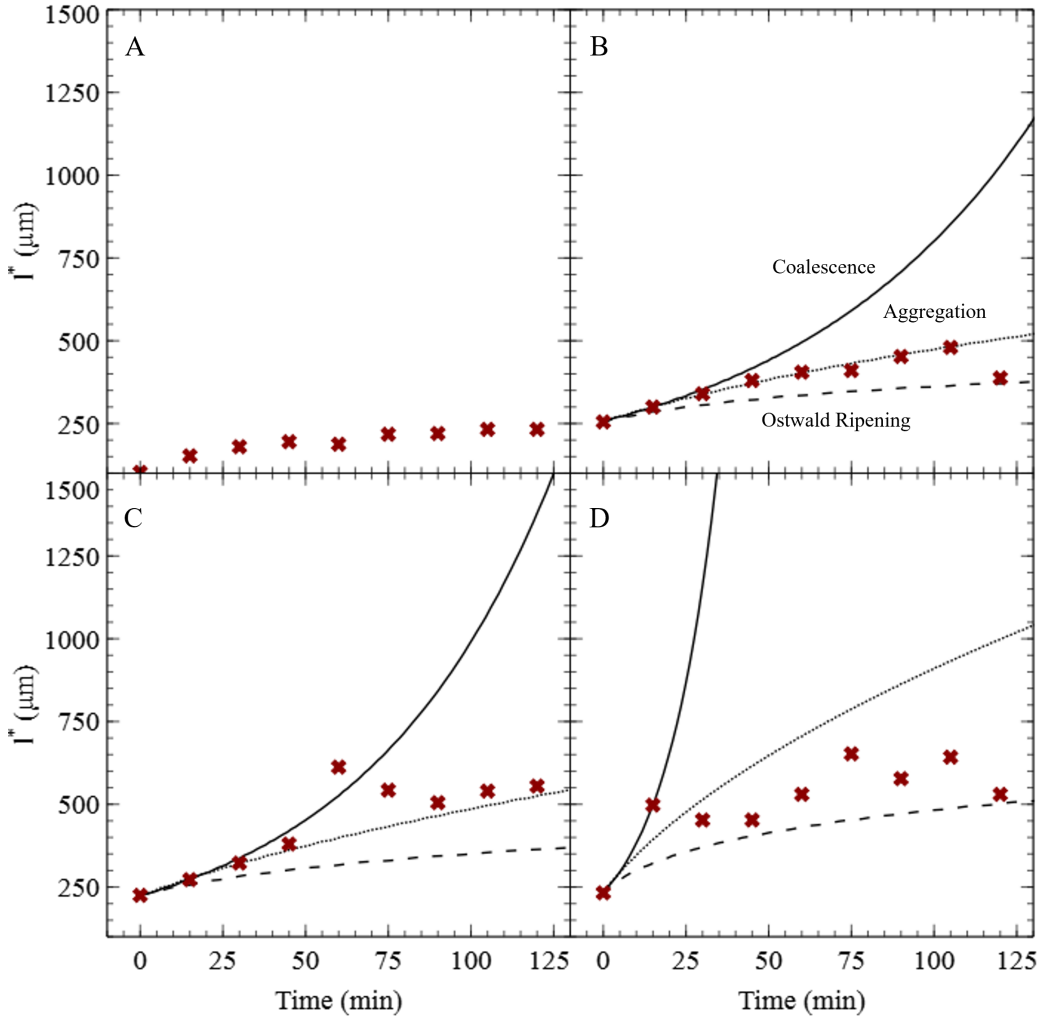

Figure 17: Tansport mean free path, l^*, as a function of lab time over 120 minutes, theoretical coalescence (solid lines), aggregation (dotted lines), and Ostwald ripening (dashed lines) kinetics, for control and emulsions prepared with GMO at 3 mM, 5 mM and 10 mM. A) l^* over lab time for a control emulsion formulation, concentration of GMO is 0 mM B) l^* over lab time for an emulsion with 3 mM GMO C) l^* over lab time for an emulsion with 5 mM GMO D) l^* over lab time for an emulsion with 10 mM GMO

Oleamide Formulations

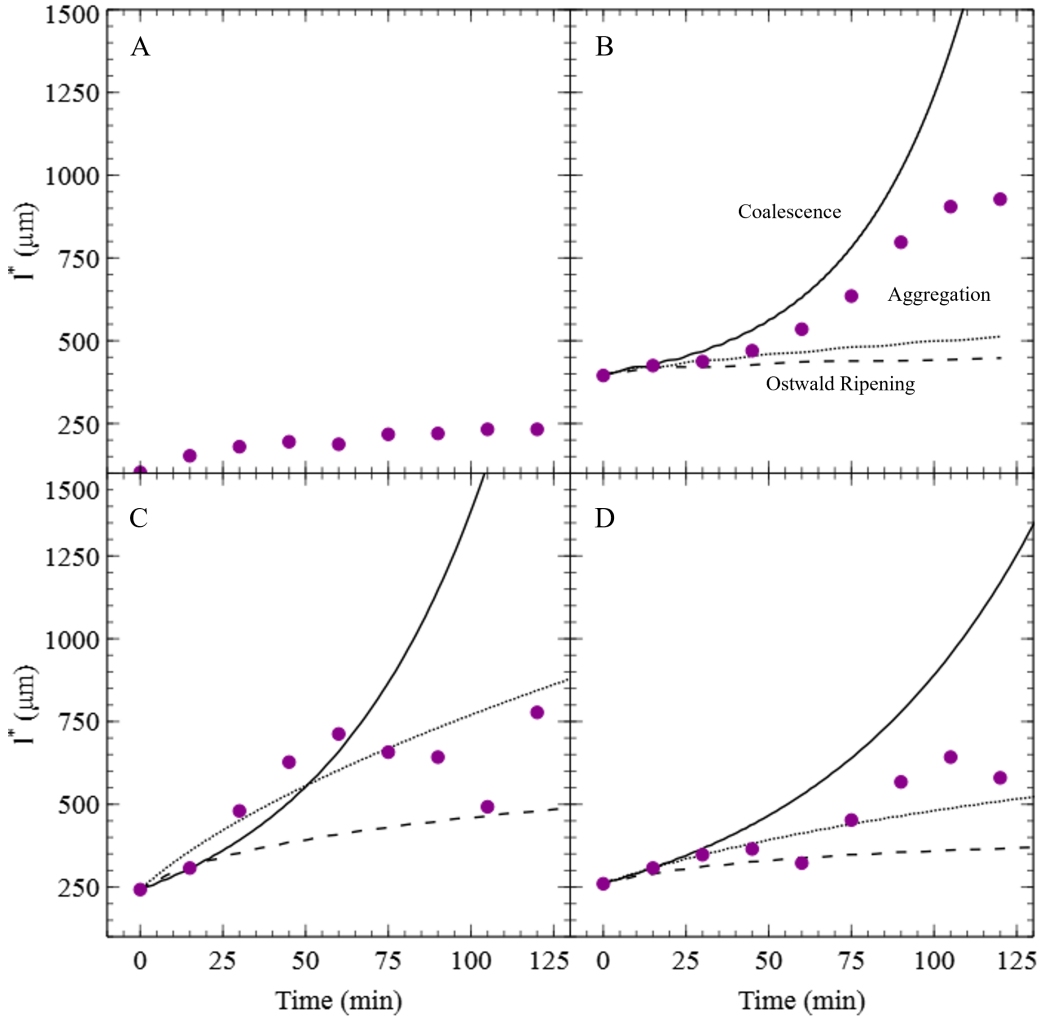

Figure 18: Transport mean free path, l^*, as a function of lab time over 120 minutes, theoretical coalescence (solid lines), aggregation (dotted lines), and Ostwald ripening (dashed lines) kinetics, for control and emulsions prepared with OA at 3 mM, 5 mM and 10 mM. A) l^* over lab time for a control emulsion formulation, concentration of OA is 0 mM B) l^* over lab time for an emulsion with 3 mM OA C) l^* over lab time for an emulsion with 5 mM OA D) l^* over lab time for an emulsion with 10 mM OA

Shown in Figures 16 to 18, increased concentration tended to lead to faster destabilization in all formulations. For emulsions formulated with GMO 17, aggregation kinetics dominated at 3 mM and larger contributions of coalescence dynamics appeared at concentrations of 5 mM and 10 mM. Emulsions formulated with GDO 16 exhibited similar destabilization behavior. However, Ostwald ripening dynamics were

apparent at the lowest concentration, followed by increasing aggregation dynamics at 5 mM, and finally coalescence dynamics contributing at the highest concentration, 10 mM. At low concentrations, emulsions containing 10 mM GDO or GMO exhibited minimal contributions of coalescence behavior, whereas those containing OA 18 demonstrated significant contributions of coalescence behavior even at the lowest concentration of 3 mM. Additionally, in contrast to GMO and GDO stabilized emulsions, OA stabilized emulsions showed a slightly increased stabilization trend with respect to concentration, as the growth of l^* was somewhat attenuated during the initial 2 hour period at 5 mM and 10 mM compared to 3 mM.

The initial l^* is thought to be indicative its ability to lower the interfacial tension, making it a good way to parameterize the emulsification capability of a surfactant. Figure 19 illustrates the initial value of l for each emulsion formulation at equivalent molar concentrations. Emulsions containing GMO exhibit a slight decrease in l^0 from 3 mM to 5 mM, followed by a consistent value at higher concentrations.

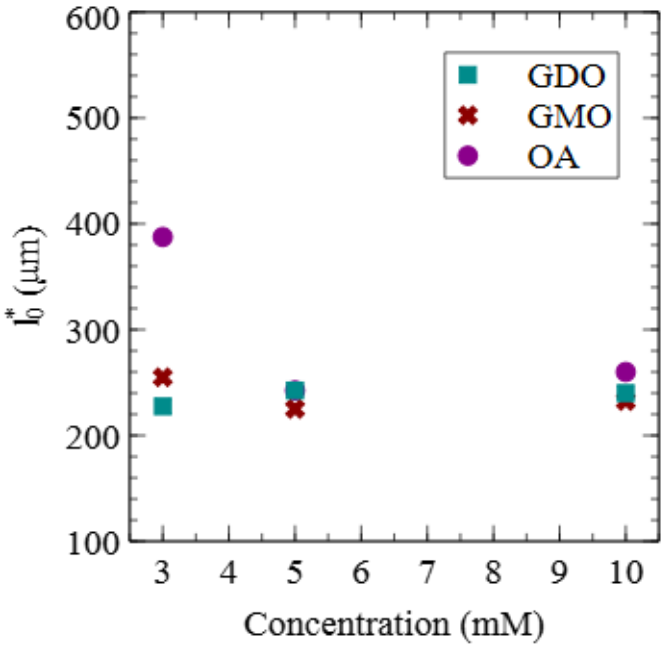

Figure 19: Effect of surfactant structure on emulsification capacity. Initial transport mean free path, l_0^*, as a function of surfactant structure and concentration.

Conversely, emulsions formulated with OA display a larger initial l^* at 3 mM, which decreases to an effectively constant value at 5 and 10 mM. At these higher concentrations, all formulations have nearly identical values of l_0^*, indicating decreasing

marginal benefit associated with increasing the surfactant concentration for the studied formulations. Furthermore, emulsions containing GMO and GDO, which have similar head groups, exhibit a comparable flat concentration profile and l_0^* values. In contrast, emulsions containing OA, which has a distinct head group, demonstrate a decreasing trend in l_0^* with a higher value at 3 mM. These results suggest that l_0^* is more strongly influenced by the surfactant head group rather than the tail group for the studied formulations.

3.2 Stabilizer Results

Table 2 presents the compiled changes in volume fraction of water (ϕ water) at 24 hours and 2 hours (expressed as percent) and percent of emulsion remaining after 24 hours for all three stabilizers. Analyzing these results in combination with l^* data help reveal previously obscured information. Figures 20-22 show the l^* analysis for the stabilizer series of experiments and will be discussed in concert with microscopy in Figures 7-9 and Table 2 data.

Er Reference	Additive	φ_{water} Initial	φ_{water} (24 hours)	φ_{water} (% Change, 2 hours)	% Emulsion (24 hours)
S1 - Control	Control (N/A)	0.15	-	-8.3%	0
S1 - A	Stabilizer 1	0.15	0.28	-3.6%	57%
S1 - B		0.15	0.21	-2.1%	75%
S1 - C		0.15	0.16	-0.1%	99%
S1 - D		0.15	0.16	0.0%	100%
S1 - E	Stabilizer 2	0.15	0.59	-6.1%	27%
S1 - F		0.15	0.63	-6.3%	25%
S1 - G		0.15	0.19	-1.3%	85%
S1 - H		0.15	0.18	-0.8%	90%
S1 - I	Stabilizer 3	0.15	0.21	-1.9%	77%
S1 - J		0.15	0.18	-1.0%	88%
S1 - K		0.15	0.19	-1.3%	85%
S1 - L		0.15	0.22	-2.3%	73%

Table 2: Changes in volume fraction of water (ϕ water) at 24 hours and 2 hours (expressed as percent) and percent of emulsion remaining after 24 hours for formulations containing stabilizers at concentrations 0.1, 0.2, 0.5, and 1.0 wt%

Formulations with Stabilizer 1

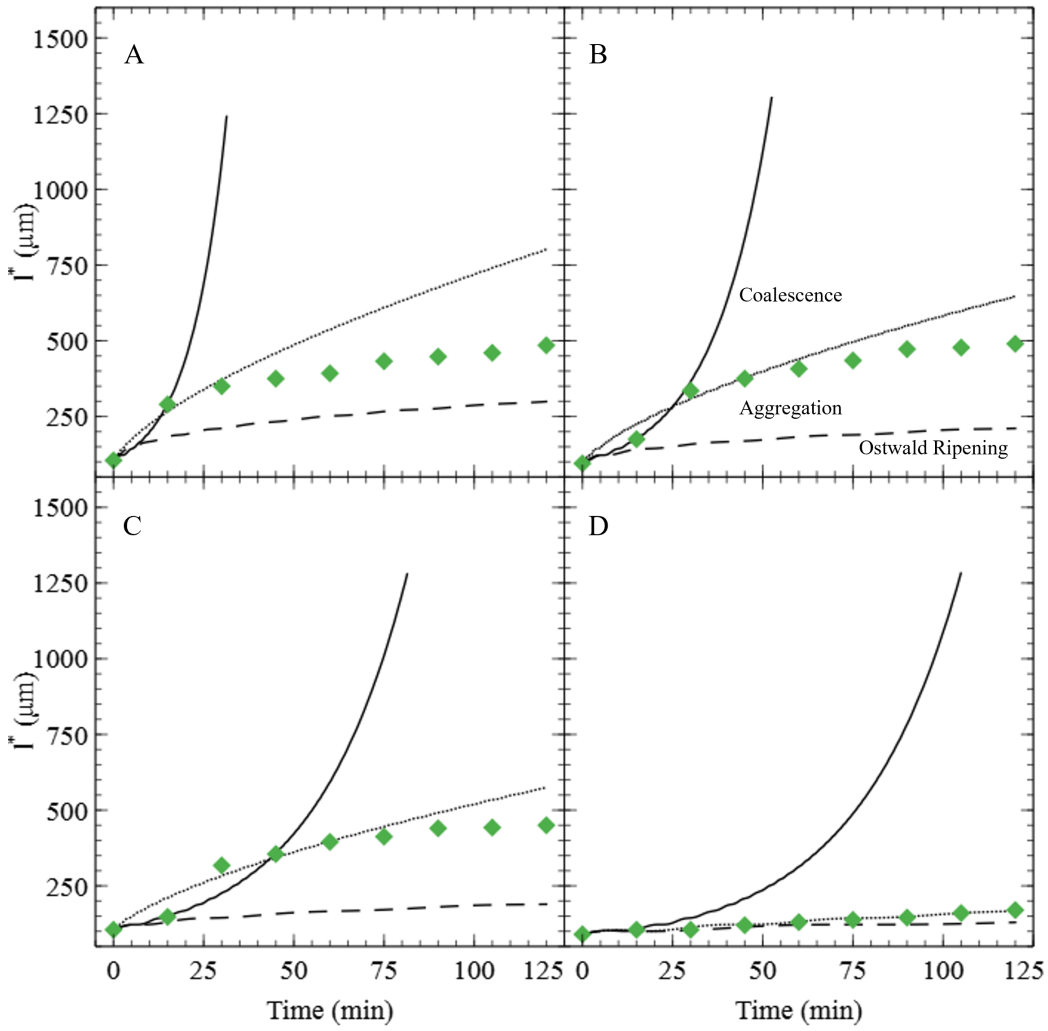

Figure 20: Transport mean free path, l^*, as a function of lab time over 120 minutes, theoretical coalescence (solid lines), aggregation (dotted lines), and Ostwald ripening (dashed lines) kinetics for emulsions prepared with Stabilizer 1 at 0.1, 0.2, 0.5, and 1.0 wt% A) l^* over lab time for an emulsion with 0.1 wt% Stabilizer 1. B) Microscopy images and l^* over lab time for an emulsion with 0.2 wt% Stabilizer 1. C) l^* over lab time for an emulsion with 0.5 wt% Stabilizer 1. D) l^* over lab time for an emulsion with 1.0 wt% Stabilizer 1.

Figure 20 shows the effect of concentration of Stabilizer 1 on the change in the transport mean free path length over 120 minutes and the volume fraction of water in the emulsion phase. In the top left panel, Figure 20A, the transport mean free path increases over 2 hours for an emulsion prepared with 0.1 wt% Stabilizer 1. Similarly, as shown in Table 2 S1-A, the volume fraction of the dispersed phase, water, increases

over time. Therefore, the change in l^* can be attributed to a growing effective average droplet size. This is also evidenced by microscopy depicted in Figure 7 row 1. Similar effects can be seen at a Stabilizer 1 concentration of 0.2 wt% (Figure 20B and Table2 S1-B), where the change in effective droplet size overcomes the increase in dispersed phase volume fraction. For a concentration of 0.5 wt%, however, Stabilizer 1 stabilizes the emulsion from macroscopic phase separation, shown in Table 2 S1-C, where the dispersed phase concentration remains nearly constant over 24 hours. Despite this macroscopic stabilization effect, l^* increases monotonically over an initial 2 hour period, implying a growing effective average droplet size and confirmed via microscopy in the micrographs shown in Figure 7 row 3. Hence, at 0.5 wt%, Stabilizer 1 may stabilize the emulsion from macroscopic separation, but does not inhibit changes in droplet size. Lastly, at a concentration of 1.0 wt%, Stabilizer 1 effectively stabilizes the emulsion with respect to macroscopic phase separation, shown in Table 2 S1-D. In comparison to concentrations of 0.1, 0.2, and 0.5 wt% Stabilizer 1 at 1.0 wt% enhances effective droplet size stability, as evidenced by a reduction in change of l^* over an initial 2 hour period and the micrographs shown in Figure 7 row 4. Despite increasing effective droplet size stability compared to lower concentrations, l^* still increased over a 2 hour period, albeit much less drastically. The ability of Stabilizer 1 to inhibit droplet size growth in the first 2 hours as a function of stabilizer concentration is confirmed by visual inspection of micrographs obtained at 120 minutes for each of the formulations studied (Figure 7 rows 1-4 column 5).

Formulations with Stabilizer 2

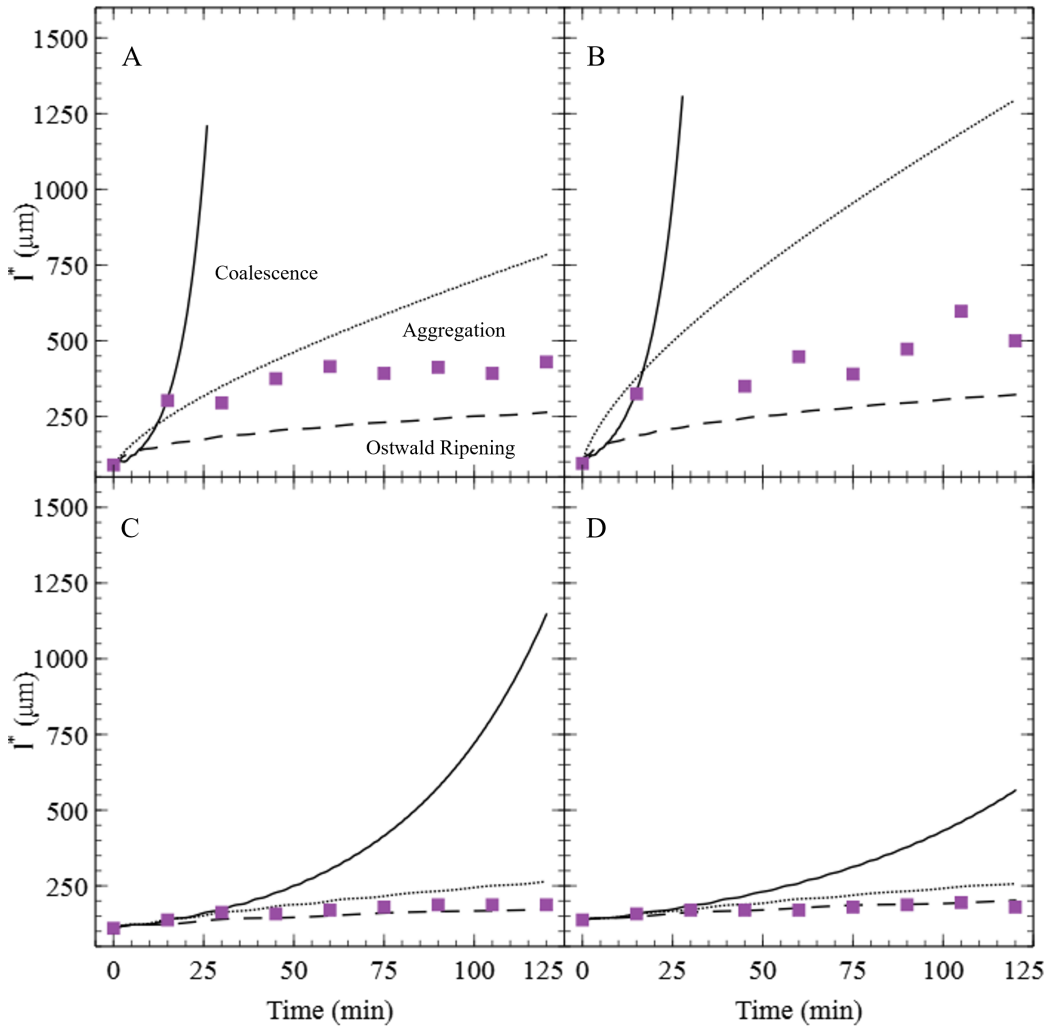

Figure 21: Transport mean free path, l^*, as a function of lab time over 120 minutes, theoretical coalescence (solid lines), aggregation (dotted lines), and Ostwald ripening (dashed lines) kinetics for emulsions prepared with Stabilizer 2 at 0.1, 0.2, 0.5, and 1.0 wt% A)l^* over lab time for an emulsion with 0.1 wt% Stabilizer 2. B) l^* over lab time for an emulsion with 0.2 wt% Stabilizer 2. C) l^* over lab time for an emulsion with 0.5 wt% Stabilizer 2. D) l^* over lab time for an emulsion with 1.0 wt% Stabilizer 2.

Stabilizer 2 appeared to be much less inhibitory to macroscopic phase separation than Stabilizer 1 did at 0.1 and 0.2 wt%, evidenced by large increases in the dispersed phase volume fraction, shown in Table 2 S1-E and -F. Additionally, at a concentration of 0.1 wt%, Stabilizer 2 showed a similar l^* profile to Stabilizer 1 (Figures 20A and 21A) over an initial 2 hour period. In contrast, at 0.2 wt%, Stabilizer 2 exhibited much

higher variability in l^* over an initial 2 hour period (Figures 20B and 21B). This implies that Stabilizer 2 performs relatively worse at macroscopic phase separation stability, as well as effective droplet size stability, compared to Stabilizer 1 at 0.1 and 0.2 wt%. Despite relatively poor stability at 0.1 and 0.2 wt%, Stabilizer 2 effectively stabilizes the emulsion with respect to macroscopic phase separation at 0.5 and 1.0 wt%, shown by de minimis changes in the dispersed phase volume fraction (Table 2 S1-G and -H). Additionally, changes in l^* are suppressed at both concentrations as shown in Figure 21C and D. Moreoever, microscopy images shown in Figure 8 rows 3 and 4 do not indicate a marked increase in effective droplet radii over the first 120 minutes. The experimental results from the ASTM D7563 test indicated a large jump in macroscopic phase stability at 0.5 wt%, which is further confirmed by a reduction in the change of l^* over an initial 2 hour period. It is suspected that the stability mechanism for Stabilizer 2 may be due to a suppression in effective droplet size changes. In contrast, Stabilizer 1 showed similar reductions in macroscopic phase suppression at 0.5 wt% but did not show suppression in effective droplet size increases. Lastly, at 1.0 wt% both stabilizers 1 and 2 effectively suppressed macroscopic phase separation, as well as, changes in effective drop size, shown in Figure 20D and Figure 21D and Table 2 S1-D and -H.

Formulations with Stabilizer 3

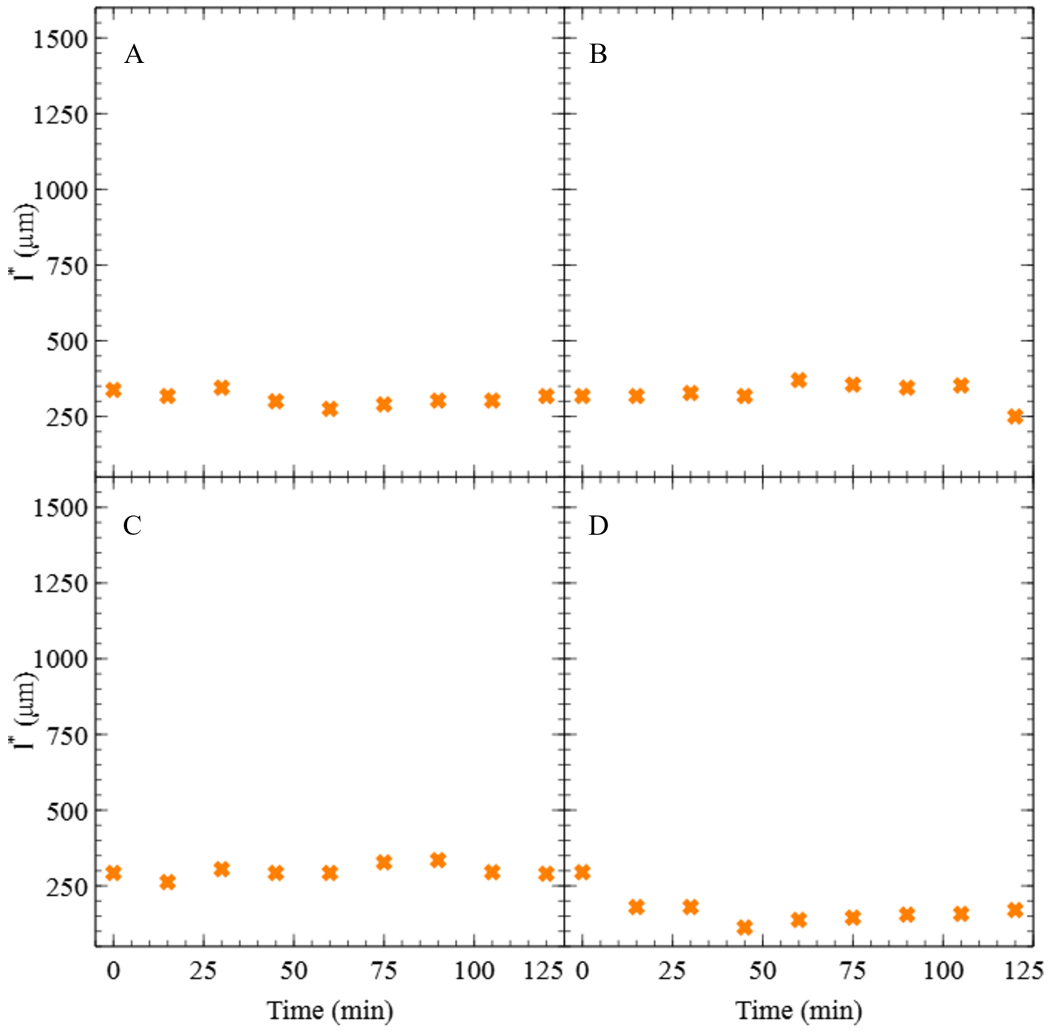

Figure 22: Transport mean free path, l^*, as a function of lab time over 120 minutes for emulsions prepared with Stabilizer 3 at 0.1, 0.2, 0.5, and 1.0 wt% A) l^* over lab time for an emulsion with 0.1 wt% Stabilizer 3. B) l^* over lab time for an emulsion with 0.2 wt% Stabilizer 3. C) l^* over lab time for an emulsion with 0.5 wt% Stabilizer 3. D) l^* over lab time for an emulsion with 1.0 wt% Stabilizer 3.

Unlike emulsions formulated with stabilizers 1 and 2, emulsions formulated with Stabilizer 3 were generally stable with regards to droplet size stability and macroscopic phase separation throughout the range of concentrations tested. At stabilizer concentrations of 0.1, 0.2, and 0.5 wt%, emulsions displayed nearly constant values of l^* over an initial 2 hour period, shown in Figure 22A, B, and C. Additionally, microscopy showed little changes in droplet size over the same two hour period (microscopy im-

ages Figure 9) and the ASTM D7563 test showed little phase separation after 24 hours (Table 2 S1-I, -J, and -K). For emulsions formulated with 1.0 wt% Stabilizer 3, l^* trended lower over the initial 2 hour period, shown in 22D. As changes in l^* are inversely proportional to $\phi(t)$, this implies that the l^* decrease overtime is due to an increase in concentration of scattering centers that outweigh even small changes in the effective droplet size of the emulsion. Therefore, it is reasonable to conclude that Stabilizer 3 is extremely effective in reducing changes in droplet size. This is further evidenced by a slight increase in the concentration of the dispersed phase (e.g., some macroscopic phase separation), shown in Figure 14B. Lastly, microscopy indicates little to no changes in droplet were observed over the initial 2 hour period. In fact, Figure 9 demonstrates that through microscopy alone, minimal information may be obtained in Stabilizer 3 formulations due to retention of highly stable small droplets in a dense emulsion.

3.3 Detergent Results

As discussed in Section 1, detergents may exhibit properties characteristic of small molecule surfactants and stabilizers or other polymeric agents. The transport mean free path l^* is largely a function of droplet sizes and concentration. Therefore, utilizing a method proposed by McMillin et al., which involves tracking (l^*) as a function of lab time, obtained via DWS analysis, and applying widely accepted theoretical models, presented in Section 1.1, to obtain mechanistic understanding of destabilization in emulsions.[18] By carefully crafting test formulations, the effect of specific detergents in overall observed destabilization mechanisms may be revealed.

Detergent 1 Formulations

The effects of Detergent 1 concentration on change in the transport mean free path length during the first 120 minutes post emulsification are depicted in Figure 23. Figure 23A, 23B, and 23C, show the transport mean free path for emulsion prepared with 0.1 wt% Detergent 1, 0.2 wt% Detergent 1, and 0.5 wt%, respectively.

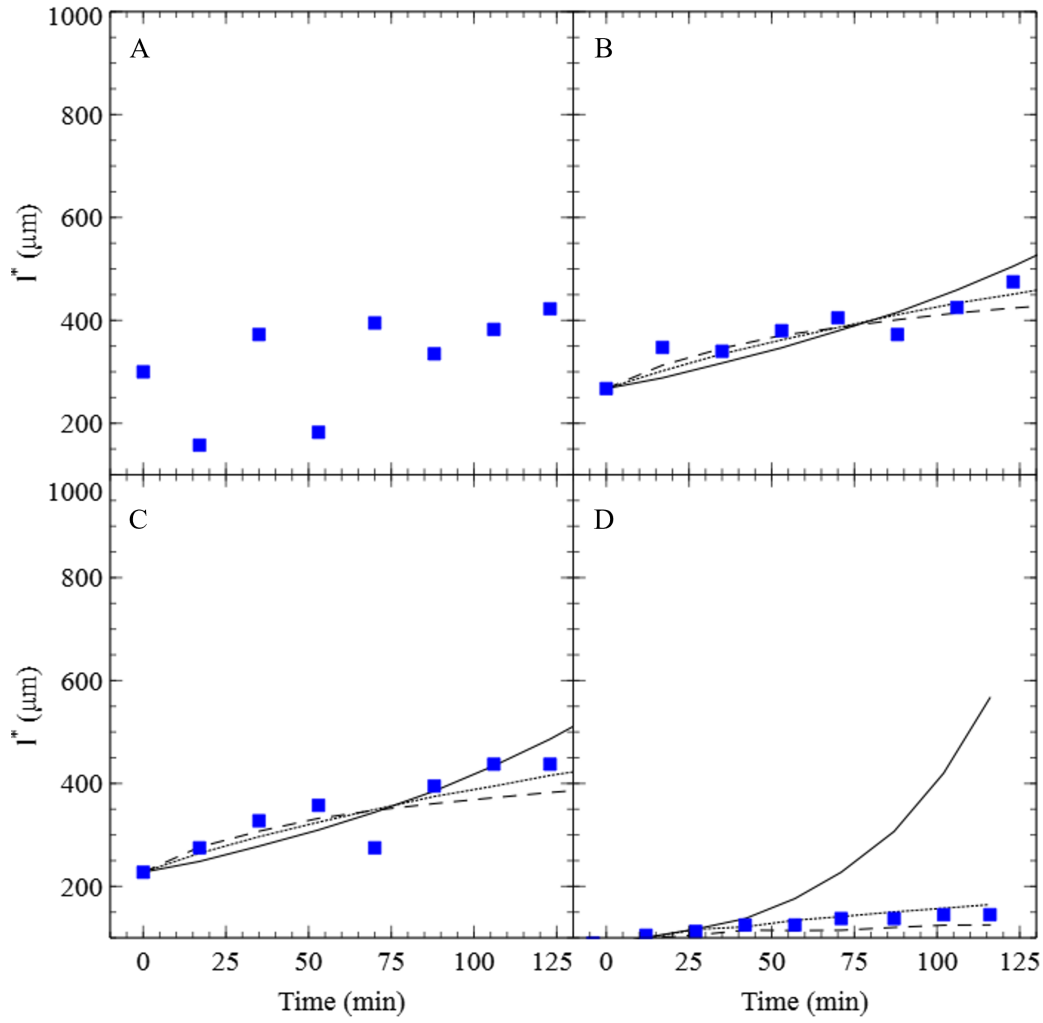

Figure 23: Transport mean free path, l^*, as a function of lab time over initial 120 minutes post emulsification, theoretical coalescence (solid lines), aggregation (dotted lines), and Ostwald Ripening (dashed lines) kinetics for emulsions prepared using detergent Detergent 1 at varying concentrations: 0.1, 0.2, 0.5, and 1.0 wt% A) l^* as a function of lab time for an emulsion with 0.1 wt% Detergent 1. B) l^* as a function of lab time for an emulsion with 0.2 wt% Detergent 1 C) l^* as a function of lab time for an emulsion with 0.5 wt% Detergent 1 D) l^* as a function of lab time for an emulsion with 1.0 wt% Detergent 1

At each of these concentrations a small gradual increase of l^* over 2 hours is observed. Further, qualitative inspection of optical microscopy obtained at 120 minutes yields minimal appreciable change as a function of detergent concentration. Similarly, as shown in Figure 15, the volume fraction of the dispersed phase, water, is approximately the same for formulations with these three concentrations. Alternatively, for Detergent 1 at 1.0 wt%, shown in Figure 23D, l^* over the initial 120 minutes post

emulsification is drastically reduced when compared to less concentrated formulations. Additionally, visual comparison of microscopy in 10 at 120 minutes shows drop size suppression as a function of detergent concentration. Once more, these observations about detergent concentration effects made through tracking l^* over the initial 120 minutes align nicely with microscopy and the ASTM data obtained at 24 hours, presented in Figure 15. However, l^* analysis provides more detailed, non-invasive, quantitative understanding of aging dynamics over initial time points.

Detergent 2 Formulations

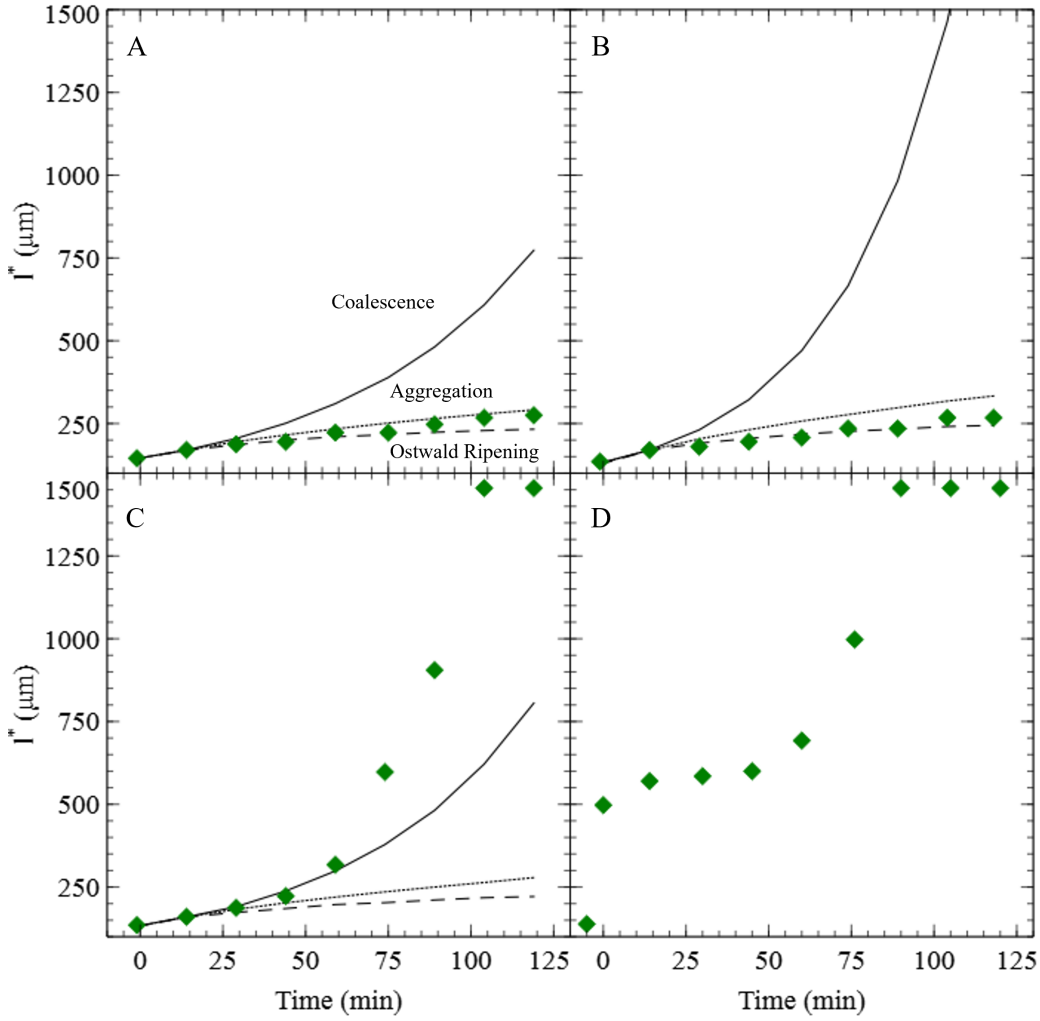

Figure 24: Transport mean free path, l^*, as a function of lab time over initial 120 minutes post emulsification, theoretical coalescence (solid lines), aggregation (dotted lines), and Ostwald Ripening (dashed lines) kinetics for emulsions prepared using detergent Detergent 2 at varying concentrations: 0.1, 0.2, 0.5, and 1.0 wt% A) l^* as a function of lab time for an emulsion with 0.1 wt% Detergent 2. B) l^* as a function of lab time for an emulsion with 0.2 wt% Detergent 2 C) l^* as a function of lab time for an emulsion with 0.5 wt% Detergent 2 D) l^* as a function of lab time for an emulsion with 1.0 wt% Detergent 2

Evolution of l^* as a function of Detergent 2 concentration during the first 120 minutes post emulsification and microscopy obtained at 120 minutes are depicted in Figure 24. Theoretical aggregation, coalescence, and OR curves are portrayed to uncover dominating mechanisms of destabilization at each of the tested concentrations: 0.1,

0.2, 0.5, 1.0 wt%. At 0.1 and 0.2 wt%, Figure 24A and Figure 24B respectively, incremental l^* changes are observed in time. Whereas, 0.5 and 1.0 wt% formulations, Figure 24C and Figure 24D respectively, exhibit step change in l^* over the first 2 hours. Furthermore, a concentration dependence at 0.5 and 1.0 wt% is revealed. These findings are consistent with ASTM data reported in Figure 15. Interestingly, analyzing l^* and comparing to theoretical models reveals a shift in the dominating mechanism of destabilization for both 0.5 and 1.0 wt%. Both emulsions show shift from aggregation (dotted line) to coalescence (solid line) in the first 120 minutes. This change was indiscernible from ASTM or Microscopy data alone.

Detergent 3 Formulations

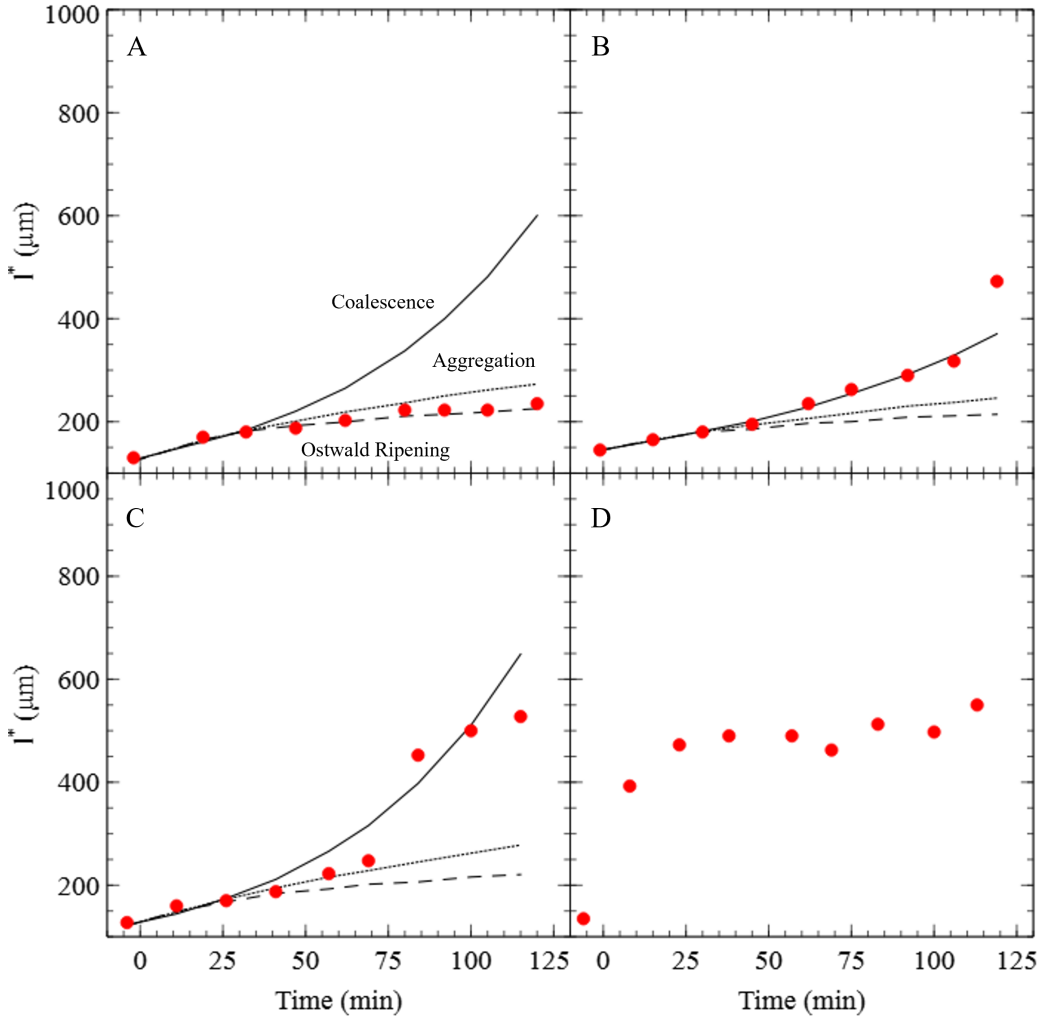

Figure 25: Transport mean free path, l^*, as a function of lab time over initial 120 minutes post emulsification, theoretical coalescence (solid lines), aggregation (dotted lines), and Ostwald Ripening (dashed lines) kinetics for emulsions prepared using detergent Detergent 3 at varying concentrations: 0.1, 0.2, 0.5, and 1.0 wt% A) l^* as a function of lab time for an emulsion with 0.1 wt% Detergent 3. B) l^* as a function of lab time for an emulsion with 0.2 wt% Detergent 3 C) l^* as a function of lab time for an emulsion with 0.5 wt% Detergent 3 D) l^* as a function of lab time for an emulsion with 1.0 wt% Detergent 3

Similar to Detergent 2, Detergent 3 exhibited a shift in dominating destabilization mechanism from aggregation to coalescence, as illustrated in Figure 25. A smooth transition of l^* values in the first 120 minutes is observed at 0.1 and 0.2 wt%, Figure 25A and Figure 25B. Whereas, at 0.5 and 1.0 wt%, Figure 25C and Figure 25D, a more

drastic jump in l^* values and overall shift of mechanism are noticed. Results from optical microscopy in Figure 12 performed at 120 minutes for all four concentrations of interest, substantiate the observed l^* behavior. In micrographs droplet size appears to increase as a function of concentration in the same way that l^* values increase with concentration of Detergent 3.

4 Discussion

4.1 Surfactants: Structural Effects

A key differentiation between the studied surfactant molecules pertains to their head and tail groups. Specifically, GDO has two carbon chains in its tail group, while the tails of OA and GMO consist of only one carbon chain (Figure 2). Moreover, the head groups of GMO and GDO are similar as they are both derived from glycerol, whereas the head group of OA is an amide. Analyzing the behavior of GMO and GDO during the initial two-hour period (Figures 16 and 17) revealed that their differences in tail groups do not significantly impact stability, as their transport mean free path length (l^*) values are comparable at all concentrations. On the other hand, as shown in Figure 18, the head group of OA leads to distinct behavior, with large contributions of coalescence dynamics observed at 3 mM concentration that gradually diminish with increasing concentration. In contrast, GMO displays opposite behavior. Thus, it is highly likely that the stability of emulsions over short periods is primarily governed by the surfactant head group. Additionally, among the studied formulations, those with glycerol-derived head groups exhibited superior short-time stabilization.

4.2 Stabilizers: Viscosity Effects

Unlike the surfactants, the stabilizer structural information was unknown. Therefore, focus was directed towards gaining a deeper comprehension of the dominating mechanisms of stabilization associated with each stabilizer. We obtained additional viscosity measurements in order to investigate effects on the bulk phase viscosity and the initial droplet size. These two parameters were determined by using the numerical inversion of Equation 6 at $l^*(t = 0)$ and are presented in Figure 26A and B, respectively.

Since the emulsions were all prepared using the same method, a small initial droplet size indicates greater surface activity. Additionally, the number density of droplets

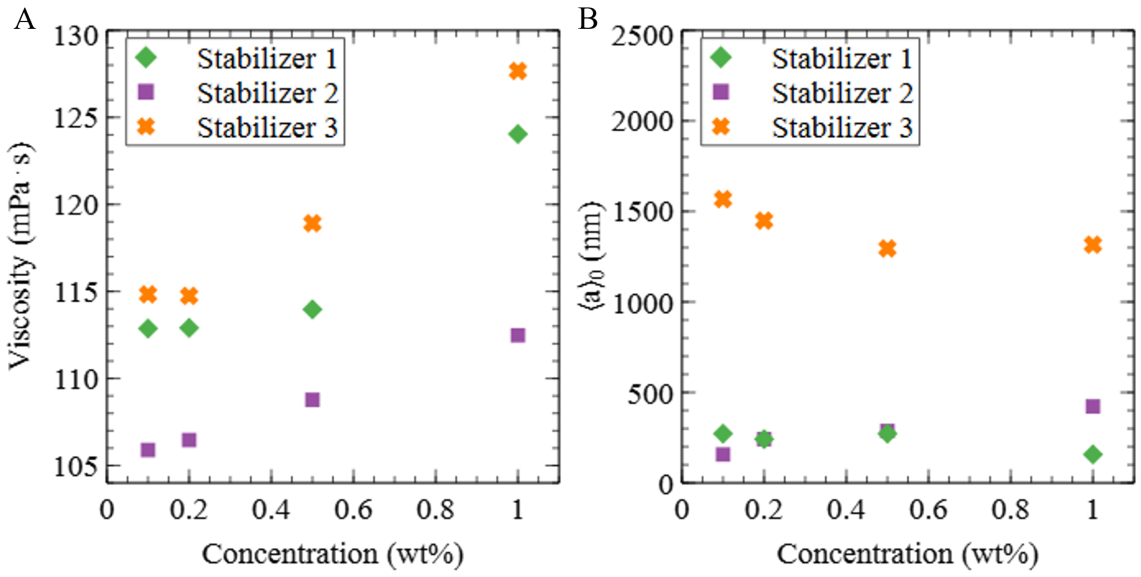

Figure 26: Viscosity and initial droplet size as a function of concentration. A) Viscosity measurements for stabilizers 1, 2 and 3 as a function of concentration B) Initial emulsion droplet size for stabilizers 1, 2, and 3, determined by Equation 6, as a function of concentration.

is inversely proportional to $\sim \langle a \rangle^3$, meaning that a smaller droplet size leads to a higher droplet density. A higher bulk phase viscosity can decrease the speed of droplet motion and the frequency of droplet-droplet interactions, such as collisions, which are necessary for aggregation and coalescence phenomena. As depicted in Figure 26B, emulsions containing stabilizers 1 and 2 exhibit notably smaller, and very similar, initial droplet sizes at all concentrations compared to those containing Stabilizer 3. Therefore, it is reasonable to conclude that stabilizers 1 and 2 primarily function at the W/O interface, while Stabilizer 3 is likely to have a preference for partitioning in the bulk phase. This is additionally corroborated by Figure 26A, which shows that adding Stabilizer 3 at all concentrations results in a greater bulk phase viscosity than adding stabilizers 1 and 2. From this, we conclude that the mode of action of Stabilizer 3 is connected to the generation of large, sluggishly moving droplets with lower densities, which reduces the frequency of collision events. Moreover, the rise in bulk phase viscosity hinders oil creaming, and as a result, reduces the occurrence of macroscopic phase separation.

Alternatively, Stabilizer 1 displays a moderate bulk phase viscosity at concentrations of 0.1 and 0.2 wt%, and at 0.5 wt% viscosity is comparable to initial concen-

trations (0.1 and 0.2 wt%) of Stabilizer 3. Finally, at 1.0 wt% the viscosity increases appreciably. Additionally, the emulsions formulated with stabilizers 1 exhibited significantly smaller initial droplet sizes than those prepared using Stabilizer 3. In terms of kinetics, emulsions prepared with 0.1 and 0.2 wt% Stabilizer 1 will have smaller, faster moving droplets at a high concentration compared to Stabilizer 3. Therefore, at these concentrations, there is likely a higher frequency of droplet collisions, which increases likelihood of aggregation or coalescence compared to Stabilizer 3. Smaller droplet sizes initially coupled with reduced viscosity, explains the reasons for both droplet instabilities and macroscopic phase separation. As noted, the viscosity of the bulk phase with 0.5 wt% Stabilizer 1 added is comparable to that of the bulk phase with 0.1 and 0.2 wt% Stabilizer 3 added. Since the initial droplet sizes are small, aggregation or coalescence may still occur due to increased concentration. During the initial 120 minute period emulsions formulated with 0.5 wt% Stabilizer 1 reach a limiting value of $\sim$ 490nm, which is similar to the nearly constant value of l^* for emulsions prepared with Stabilizer 3 at 0.1 and 0.2 wt% ($\sim$ 265nm). Thus, as the viscosity is similar, we predict that emulsions containing 0.5 % Stabilizer 1 will undergo aggregation and/or coalescence resulting in sizes comparable to the initial droplet sizes of emulsions made with 0.1 and 0.2 wt% Stabilizer 3 before viscosity increases retard further ageing. Moreover, owing to the surface activity of Stabilizer 1, oil creaming is greatly suppressed, and macroscopic phase separation is substantially reduced as evidenced by Figure 14A.

Lastly, when comparing the emulsions prepared with Stabilizer 2 to those prepared with Stabilizer 1, initial droplet sizes were similar for all concentrations investigated. As noted previously, these initial sizes were appreciably smaller than initial droplet sizes for emulsions prepared with Stabilizer 3. Furthermore, the bulk phase viscosities measured with 0.1 and 0.2 wt% Stabilizer 2 formulations were much lower than the comparable Stabilizer 1 and 3 formulations. As shown in Figure 14B, emulsions prepared with these concentrations of Stabilizer 2 also exhibited the largest macroscopic phase separation. Additionally, l^* analysis at these two concentrations, depicted in Figure 21A and B, show obvious large changes in droplet sizes during the initial 120 minutes of study. Therefore, the low viscosity coupled with small, faster moving droplets likely increased frequency of droplet collisions and aided in the formation of larger droplets and aggregates. Subsequently, these larger sized droplets or clusters could move more unreservedly through the bulk phase, escalating the speed of macroscopic phase separation. However, formulations containing 0.5 and 1.0 wt% Stabilizer

2, exhibited lower viscosity than with 0.5 or 1.0 wt% Stabilizer 1 or 3. In spite of this, l^* was highly attenuated over the initial 120 minute period (Figure 21C and D). The l^* suppression and pronounced interfacial activity, represented by initial droplet sizes in Figure 26B, support that Stabilizer 2 most likely acts sterically to hinder aggregation and/or coalescence at higher concentrations. Furthermore, it could potentially increase interfacial viscosity, thereby decelerating droplets and reducing the frequency of collisions.

4.3 Detergents: Comparing Classes of Additives

As mentioned in Section 1 during emulsification surfactants lower the interfacial tension between the dispersed and continuous phase and are responsible for decreasing the total energy associated with increasing interfacial area. It is commonly hypothesized that surfactants retard thermodynamic driving forces that result in destabilization.[8] Additionally, surfactants may modify the interface to reduce aggregation and coalescence thereby slowing emulsion destabilization due to increased droplet size. Additional possible methods of surfactant stabilization include increasing interfacial viscosity to reducing thermal motion and settling, sterically hindering droplets to prevent coalescence, and amplifying electrostatic repulsion between droplets.[6,9] Alternatively, polymeric stabilization of W/O emulsions occurs by two primary mechanisms: momentum transfer boundary condition modification at the interface and steric hindrance.[5,10] Regardless of mechanism, polymers generally cause increased viscosity, decreasing the speed of droplet diffusion.[10] Additionally, the polymer can preferentially partition in either the bulk phase or the dispersed phase. Of note, these phenomena and others may occur simultaneously. For example, bulk and interfacial viscosity modification often happen concurrently. As reported in the work of McMillin et al.[18] DWS, kinetic modeling, ASTM testing and optical microscopy may be used to elucidate mechanisms of action in emulsion destabilization for both surfactants and polymers. In prior studies, polymers tended to exhibit suppression of l^* and rapid increase in the stability at some critical concentration. Whereas, small molecule surfactants showed a maxima stability, evidenced through ASTM testing, and gradual destabilization in l^*. As previously noted, detergents seem to exhibit hybridized behavioral characteristics resembling both surfactants and polymers. Therefore, we identify and discuss mechanisms of action causing destabilization in emulsion formulations containing varying concentrations of three specific sulfonate detergents Detergent 1, Detergent 2, and Detergent 3 with an identical method of DWS analysis

developed and reported by McMillin et al..[18] Additionally, we compare the detergent behavior to trends observed with surfactants and stabilizers in an effort to better categorize these functional additives.

It is shown by McMillin et al. that the efficiency of a typical emulsification can be represented by the ratio of energy input, E_{in}, to the sum of all energy input for the creation of interfacial area, $E_A = \gamma A$: $\eta = \frac{\gamma A}{E_{in}}$, assuming the initial interfacial area is negligible.[18] Substituting $A = n4\pi a^2$ and $n = \phi/(4/3\pi a^3)$ into efficiency expression and rearranging results in an initial droplet size equation as follows:

$$a = \frac{3\gamma\phi_0}{\eta E_{in}} \tag{8}$$

In Equation 8, ϕ_0, η, and E_{in} are all constant, so the initial drop radius is directly proportional to the interfacial tension, γ. Similarly, from Equation 6, the initial l^* indicates the ability of a surfactant or other stabilizer to lower the interfacial tension. Figure 27 shows the initial l^* for each emulsion formulation examined at concentrations 0.1, 0.2, 0.5, and 1.0 wt%.

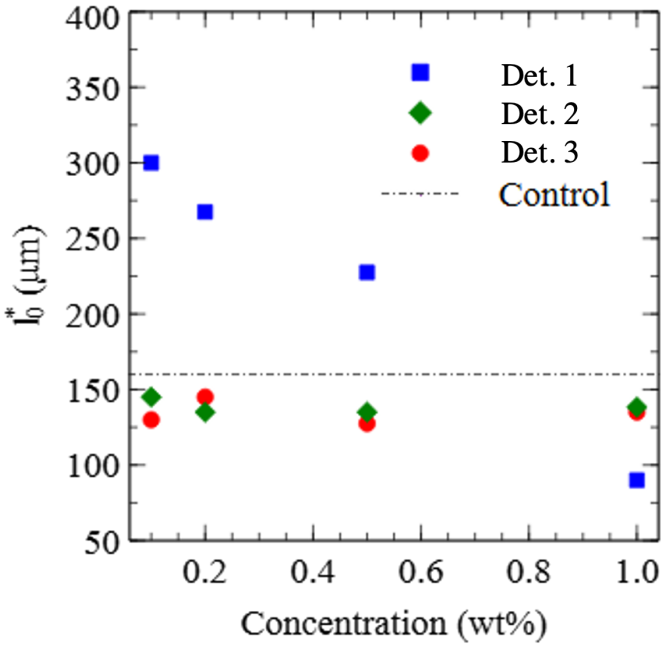

Figure 27: Initial transport mean free path, l_0^*, as a function of detergent concentration for emulsion samples prepared with Detergent 1, Detergent 2, and Detergent 3 at 0.1, 0.2, 0.5, and 1.0 wt% with comparison to a control formulation.

For emulsions prepared with Detergent 1, l_0^* is strongly decreasing as a function of

concentration. In contrast, initial l^* values for emulsions prepared with Detergent 3 and Detergent 2 are very similar to the control and essentially remain constant across all tested concentrations. This indicates potential diminishing return on the emulsification ability associated with increasing Detergent 3 and Detergent 2 concentrations.

Potential mechanisms of destabilization for each detergent were further investigated, by modeling three common droplet kinetic ageing processes and plotting them with l^* values extracted from DWS, shown by Figures 23 24 and 25. To fit models to the data, two initial l^* points were converted to radii using Equation 6, regressed with Eqs. 2 and 3, and then projected over the 120 minute time period. The 24 hour volume fraction change was linearized and used as an input to the model equations. l^* decreased appreciably for emulsions prepared with Detergent 1 as a function of concentration and at 1.0 wt% droplets displayed nearly complete aggregation kinetics (Figure 23D), this trend strongly resembles other stabilizer behavior as reported by McMillin et al.[18] Emulsions prepared with Detergent 2 at 0.1, 0.2 wt% exhibited behavior in line with aggregation kinetics, but at 0.5 wt% and 1.0 wt% formulations showed a sharp transition towards coalescence like behavior around 60 minutes post emulsification (Figure 24). Similar to Detergent 2 behavior, Detergent 3 formulations exhibited increasing l^* as a function of concentration, a more pronounced shift from aggregation to coalescence kinetics at later time points was observed with 0.5 and 1.0 wt% formulations (Figure 25C/D). However, Detergent 3 differs from Detergent 2 at 0.2 wt%, as it exhibits a smooth transition from aggregation to coalescence kinetics (Figure 25B). Establishing which kinetic model is most aligned with l^* data may often seem ambiguous and difficult to discern, thereby making determination of a dominating mechanism difficult. For example, in Figure 24B Detergent 2 at 0.2 wt% appears to either be dominated by aggregation or OR. However, OR kinetics typically occur over longer time durations, therefore it is suspected that aggregation is the dominating mechanism of action in destabilization during these first 120 minutes. AS is true with any method, limitations exist. However, the DWS analysis provides significantly more detailed mechanisitc information than any other traditional techniques.

After analyzing plots of l^* over initial 120 minutes post emulsification, kinetic curves, initial l^* value trends, and ASTM data for formulations prepared with a range of detergent concentrations we suspect that Detergent 3 and Detergent 2 are more likely to partition and be active at the interface. Therefore, they more strongly mimic surfactant like effects than Detergent 1. Detergent 1 showed drastic stability increase after 0.5 wt%, as depicted in both ASTM and l^* data (Figures 15 and 23D). This

drastic stability change at a critical concentration is indicative of polymer or stabilizer like behaviors such as partitioning in the bulk phase and modifying the viscosity. However, it is interesting that initial l^* value decreased strongly as a function of concentration. This is perhaps one of the best examples of how detergents exhibit a mixture of both surfactant and polymer like behavior. Table 3 provides a brief summary of detergent properties and behaviors for the three sulfonate detergents investigated in this work.

	Detergent 1	Detergent 2	Detergent 3
Stability	-Rapid increase in stability at critical conc. (0.5 wt%)	-Smooth ASTM stability profile -Maxima in stability	-Smooth ASTM stability profile -Maxima in stability
l* Trends	-Suppression of l*	-Increasing destabilization in l*	-Increasing destabilization in l* -Initial l* similar to control
Dominating Mode of Stabilization	*Polymer* -Viscosity modifier -Bulk phase partitioning	*Surfactant* -Interfacial partitioning	*Surfactant* -Interfacial partitioning

Table 3: Summary table for three sulfonate detergents: Detergent 1, Detergent 2, and Detergent 3 investigated via DWS analysis, microscopy, and ASTM-D7563

The same three methods of analysis were employed including DWS, microscopy, and the standard ASTM-D7563 test, and when reviewing results for this portion of the project specific attention was paid to comparing the behavior of detergents to those of small molecule surfactants and stabilizers. As discussed previously, in most cases the detergents exhibited hybridized characteristics. However, generally speaking Detergent 1 appears to behave more dominantly like a stabilizer. Whereas, Detergent 2 and Detergent 3 seem to act most similar to surfactants. This additional knowledge pertaining to mechanistic behaviors of differing classes of molecules may significantly improve optimization of formulations involving these detergents.

5 Conclusion

In this project, nine molecules belonging to three different categories of commonly used additives were investigated at various concentrations. These molecules included Surfactants: GDO, GMO, OA; Stabilizers: 1, 2, 3; and Detergents: Detergent 1, Detergent 2, Detergent 3. As previously mentioned, varying information pertaining to structural and chemical properties were provided about the nine additives prior to experimentation. However, through consistent formulation and organized experimental design, trends were revealed, and dominating mechanisms of destabilization as emulsions aged in time were established. Additionally, comparison across classes of additives was possible, and behavior of sulfonate detergents was broken down and further classified. It was demonstrated that insights into destabilization mechanisms otherwise unattainable through traditional methods alone were possible via non-invasive DWS methods, optical microscopy, and standard ASTM-D7563 testing. All this possible, in spite of minimal knowledge associated with chemical properties and molecular structure. DWS may be used as a formulation tool to streamline the experimental process, provide valuable data, and gain insights into the mechanisms of emulsion formation and destabilization.[18,27] The methods used in this work may have practical applications for formulating products in a wide array of industries particularly the automotive lubricating industry where formation and stabilization of emulsions is critical to enhancing combustion engine efficiency and performance.[12]

References

[1] A Comprehensive Review on Emulsions and Emulsion Stability in Chemical and Energy Industries. *The Canadian Journal of Chemical Engineering*

[2] Wong, P. T.; Wang, S. H.; Ciotti, S.; Makidon, P. E.; Smith, D. M.; Fan, Y.; Schuler, C. F.; Baker, J. R. Formulation and Characterization of Nanoemulsion Intranasal Adjuvants: E ffects of Surfactant Composition on Mucoadhesion and Immunogenicity. *Molecular Pharmaceutics* **2014**,

[3] Appelqvist, I. A. M.; Golding, M.; Vreeker, R.; Zuidam, N. J. Emulsions as delivery systems in foods Stabilization and destabilization of emulsion systems Emulsion stabilization. In *Encapsulation and Controlled Release Technologies in Food Systems*, 2nd ed.; Lakkis, J. M., Ed.; John Wiley and Sons Ltd, 2019; Chapter 6, p 177.

[4] Emulsion Formation and Stabilization by Biomolecules: The Leading Role of Cellulose. *Polymers (Basel)* **2019 Sep 26**, *11(10):1570*.

[5] Zhu, Q.; Pan, Y.; Jia, X.; Li, J.; Zhang, M.; Yin, L. Review on the Stability Mechanism and Application of Water-in-Oil Emulsions Encapsulating Various Additives. *Comprehensive Reviews in Food Science and Food Safety* **2019**, *18*, 1660–1675.

[6] Yuwen Ting, S.-C. H., Jing-Yu Hu Techniques and methods to study functional characteristics of emulsion systems. *Journal of Food and Drug Analysis Volume 25, Issue 1*, 16–26.

[7] McClements, D. J. Nanoemulsions versus microemulsions: terminology, differences, and similarities. *Soft matter* **2012**, *8*, 1719–1729.

[8] Zembyla, M.; Murray, B. S.; Sarkar, A. Water-in-oil emulsions stabilized by surfactants, biopolymers and/or particles: a review. *Trends in Food Science and Technology* **2020**, *104*, 49–59.

[9] Jansen, K. M. B.; Agterof, W. G. M.; Mellema, J. Viscosity of surfactant stabilized emulsions. *Journal of Rheology* **2001**, *45*, 1359–1371.

[10] Sweeta Akbari,; Abdurahman Hamid Nour, Emulsion types, stability mechanisms and rheology: A review. *International Journal of Innovative Research and Scientific Studies* **2018**, *1*, 14–21.

[11] Correlation Study of Physicochemical, Rheological, and Tribological Parameters of Engine Oils. *Advances in Tribology*

[12] Rizvi, S. Q. A. A Comprehensive Review of Lubricant Chemistry, Technology, Selection, and Design. **2009**,

[13] Devlin, M. T. Common properties of lubricants that affect vehicle fuel efficiency: a North American Historical Perspective. *Lubricants* **2018**, *6*, 68.

[14] Reitz RD, P. R., Ogawa H IJER editorial: The future of the internal combustion engine. *International Journal of Engine Research* 3–10.

[15] Nassar A.M., E.-s. R. e. a., Ahmed N.S. Preparation and evaluation of the mixtures of sulfonate and phenate as lube oil additives. *Int J Ind Chem 8*, 383–395.

[16] International, A. Standard Test Method for Evaluation of the Ability of Engine Oil to Emulsify Water and Simulated Ed85 Fuel. 2016; `https://www.astm.org/d7563-10r16.html`.

[17] Monitoring the Early Stages of Formation of Oil–Water Emulsions Using Flow Cytometry. *Langmuir* **2022**, 62–71.

[18] McMillin, R. E.; Orsi, D.; Cristofolini, L.; Ferri, J. K. Particle sizing in non-dilute dispersions using diffusing wave spectroscopy with multiple optical path lengths. *Colloid and Interface Science Communications* **2022**, *49*, 100641.

[19] Emulsion ageing: effect on the dynamics of oil exchange in oil-in-water emulsions. *soft matter* **Oct 2012**, *9*, 48–59.

[20] Kettler, E.; Müller, C. B.; Klemp, R.; Hloucha, M.; Döring, T.; Von Rybinski, W.; Richtering, W. Polymer-stabilized emulsions: Influence of emulsion components on rheological properties and droplet size. *Progress in Colloid and Polymer Science* **2007**, *134*, 90–100.

[21] Euston, S. R.; Finnigan, S. R.; Hirst, R. L. Kinetics of droplet aggregation in heated whey protein-stabilized emulsions: Effect of polysaccharides. *Food Hydrocolloids* **2002**, *16*, 499–505.

[22] De Smet, Y.; Deriemaeker, L.; Parloo, E.; Finsy, R. On the determination of Ostwald ripening rates from dynamic light scattering measurements. *Langmuir* **1999**, *15*, 2327–2332.

[23] Euston, S. R.; Finnigan, S.; Hirst, R. Aggregation kinetics of heated whey protein-stabilized emulsions. *Food Hydrocolloids* **2000**, *14*, 155–161.

[24] Weitz, D. A.; Pine, D. J. Diffusing Wave Spectroscopy. In *Dynamic Light Scattering: The Method and Some Applications*, 1st ed.; Clarendon Press, 1993; Chapter 16.

[25] Rojas, L. F.; Bina, M.; Cerchiari, G.; Escobedo-Sánchez, M. A.; Ferri, F.; Scheffold, F. Photon path length distribution in random media from spectral speckle intensity correlations. *European Physical Journal: Special Topics* **2011**, *199*, 167–180.

[26] Fahimi, Z.; Aangenendt, F. J.; Voudouris, P.; Mattsson, J.; Wyss, H. M. Diffusing-wave spectroscopy in a standard dynamic light scattering setup. *Physical Review E* **2017**, *96*, 062611.

[27] Lorusso, V.; Orsi, D.; Salerni, F.; Liggieri, L.; Ravera, F.; McMillin, R.; Ferri, J.; Cristofolini, L. Recent developments in emulsion characterization: Diffusing Wave Spectroscopy beyond average values. *Advances in Colloid and Interface Science* **2021**, *288*, 102341.

[28] Ishimaru, A. Chapter 9 - Diffusion Approximation. In *Wave Propagation and Scattering in Random Media*; Ishimaru, A., Ed.; Academic Press, 1978; pp 175–190.

[29] Mengual, O.; Meunier, G.; Cayré, I.; Puech, K.; Snabre, P. TURBISCAN MA 2000: Multiple light scattering measurement for concentrated emulsion and suspension instability analysis. *Talanta* **1999**, *50*, 445–456.

[30] Sudiarta, I. W.; Chýlek, P. Mie scattering by a spherical particle in an absorbing medium. *Applied Optics* **2002**, *41*, 3545.

[31] Hulst, H. C.; van de Hulst, H. C. *Light scattering by small particles*; Courier Corporation, 1981.

[32] Wu, X.; Pine, D.; Chaikin, P.; Huang, J.; Weitz, D. Diffusing-wave spectroscopy in a shear flow. *JOSA B* **1990**, *7*, 15–20.

[33] Oliveira, F. A.; Ferreira, R. M. S.; Lapas, L. C.; Vainstein, M. H. Anomalous Diffusion: A Basic Mechanism for the Evolution of Inhomogeneous Systems. *Frontiers in Physics* **2019**, *7*.

[34] Surfactants: Recent advances and their applications. *Composites Communications* **2020**, *22*.

[35] Polymeric stabilized emulsions: steric effects and deformation in soft systems. *Langmuir 28(10):4599-604*.

[36] Dastjerdi, Z.; Cranston, E. D.; Berry, R.; Fraschini, C.; Dubé, M. A. Polymer Nanocomposites for Emulsion-Based Coatings and Adhesives. *Macromolecular Reaction Engineering* **2019**, *13*, 1800050.

[37] Polymeric surfactants in disperse systems. *Adv Colloid Interface Sci.* **2009**, 281–99.

[38] The effect of over-based calcium sulfonate detergent additives on white etching crack (WEC) formation in rolling contact fatigue tested 100Cr6 steel. *Tribology International* **2019**, *133*, 246–262.

[39] *Colloids and Surfaces A: Physicochemical and Engineering Aspects* **2004**, *238*, 151–158.

[40] Schätzel, K. Noise on photon correlation data. I. Autocorrelation functions. *Quantum Optics: Journal of the European Optical Society Part B* **1990**, *2*, 287–305.